Nano Research

Open Access

Review Article

# Bionic hierarchically ordered structured organic–inorganic composites (BOICs): From materials manufacturing to tissue regeneration engineering

Shuxian Zhou[1], Haiyan Wu[1], Yadong Yu[2], Jue Shi[1], Zhijian Xie[1]✉, and Wenjing Jin[1]✉

[1] *Stomatology Hospital, School of Stomatology, Zhejiang University School of Medicine, Zhejiang Provincial Clinical Research Center for Oral Diseases, Zhejiang Key Laboratory of Oral Biomedical, Zhejiang-Singapore International Joint Laboratory of Oral Bioengineering, Zhejiang Clinovation Pride, Hangzhou 310000, China*

[2] *School of Chemical Engineering and Technology, Tianjin University, Tianjin 300072, China*

**Cite this article:** *Nano Research*, **2026**, *19*, 94908420. https://doi.org/10.26599/NR.2026.94908420

**ABSTRACT:** Biominerals, such as bones and teeth, are typically natural organic–inorganic composites characterized by hierarchically ordered structures and exceptional mechanical properties. In contrast, synthetic organic–inorganic composites exhibit inferior structural order, mechanical performance, and bioactivity, which restricts their clinical applicability. Researchers have been inspired to precisely regulate the integration and spatial arrangement of organic matrix (e.g., collagen, chitosan) and inorganic units (e.g., calcium phosphate) via mimicking the process of biomineralization to fabricate bionic hierarchically ordered structured organic–inorganic composites (BOICs). These BOICs demonstrate distinguished mechanical properties and biocompatibility, and even perform novel functions, including the bionic bone scaffolds for hard tissue regeneration, bionic mandibular scaffolds for gradient repair, and even as substitutes for tendons. Furthermore, BOICs offer opportunities to study the structural ordering and mechanical properties of artificially enhanced organic–inorganic composites and their effects on biological behaviors of cells. This review systematically summarizes the hierarchically ordered structures and mechanical characteristics of bones and teeth, details current BOICs construction strategies, and highlights their applications in tissue repair. Finally, the current challenges in the development and clinical implementation of BOICs are discussed, with the aim of stimulating innovative ideas and encouraging further developments in tissue regeneration engineering.

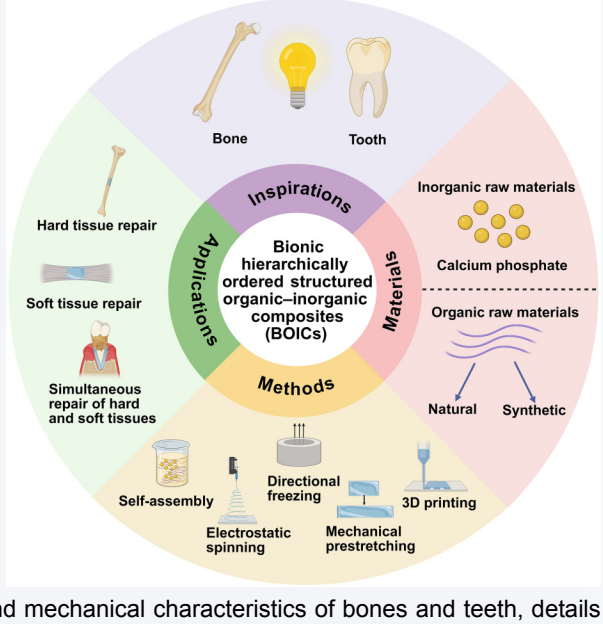


**KEYWORDS:** bioinspired materials, hierarchically ordered structure, organic–inorganic composites, tissue regeneration engineering

## 1 Introduction

In nature, numerous living systems form biogenic minerals or biominerals, which are multifunctional hierarchically ordered structured composites containing an organic matrix and inorganic minerals, such as bones, teeth, pearls, and antlers [1–3]. From a materials science perspective, organic molecules exhibit softness, compliance, and fracture resistance, whereas inorganic crystals are characterized by high hardness and brittleness. Strikingly, biominerals synergize the advantages of different matrices to achieve a combination of contradictory properties such as high strength and toughness. The exceptional properties of natural organic–inorganic composites inspire scientists to mimic biological

**Received:** November 10, 2025; **Revised:** January 6, 2026
**Accepted:** January 8, 2026

✉Address correspondence to Zhijian Xie, xzj66@zju.edu.cn; Wenjing Jin, wjjin@zju.edu.cn

structures and focus on fabricating bionic hierarchically ordered structured organic–inorganic composites (BOICs) [4, 5]. Currently, various tooth-like, bone-like, and shell-like bionic materials with diverse structures have been synthesized, drawing on bionic approaches based upon the well-established biomineralization mechanisms [6, 7]. Among these, the unique biological tissue structures of human bones and teeth have received significant attention. Due to their excellent mechanical strength and biological regulation functions, bone-like and tooth-like multifunctional bioinspired materials have wide application prospects in tissue regeneration engineering.

The organic–inorganic interactions at the molecular scale and the oriented structures are two essential factors for the mechanical properties and biological functions of BOICs [8, 9]. Natural organic–inorganic composites usually form copolymers through strong covalent bonds with building blocks that involve sub-nanometer-sized protein fragments and hydroxyapatite (HAP) crystals. For example, bone is composed of collagen fibers made up of type I collagen molecules (300 nm long and 1.5 nm in diameter) and HAP ($Ca_{10}(PO_4)_6(OH)_2$) nanocrystals (plate-like, 50 nm × 25 nm in size and 1.5–4 nm in thickness) [10]. Inspired by *in vivo* collagen mineralization, great advances have been made in fabricating BOICs by using natural and synthetic polymers, such as alginates, cellulose, and gelatin-methacryloyl (GelMA), to imitate collagen as organic building blocks. Besides, various nanostructured calcium phosphates (NCaPs) with different sizes and morphologies were developed as inorganic building blocks for BOICs. However, the mechanical properties and biological function of synthetic organic–inorganic composites are significantly poorer than those of biominerals. The susceptibility of synthetic HAP to aggregation often results in an interphase boundary between organic and inorganic phases in hybrid composites, which limits material mechanical performance enhancement and structural organization. It has been well-documented that decreasing the size of the inorganic matrix and its aggregation in composites can effectively enhance material properties, especially for mechanical characteristics [11]. Recently, "inorganic ionic polymerization" synthesized calcium phosphate oligomer (CPO, size ~ 1 nm) has been proposed to produce homogenous organic–inorganic composites with marvelous structures and exceptional mechanical properties [12, 13]. Meanwhile, various synthetic methods have been developed for constructing BOICs, including self-assembly, electrostatic spinning, directional freezing, mechanical prestretching, and three-dimensional (3D) printing.

Due to their distinguished hierarchically ordered structures and superior mechanical performance, BOICs play an important role in tissue regeneration engineering, including large-scale hard tissue repair (bone and tooth), soft tissue repair (ligament and tendon), and simultaneous repair of hard and soft tissues (periodontal and joint tissue) [14]. These materials typically serve as tissue substitutes or extracellular matrix (ECM) mimics during the tissue-regeneration process by providing suitable mechanical support for host cell behavior, such as proliferation, migration, and differentiation [15]. It has been demonstrated that excellent biocompatibility and bionic characteristics endow BOICs with diverse regenerative characteristics, thereby supporting cell adhesion and growth. Additionally, these materials effectively regulate the inflammatory microenvironment, osteogenic signaling pathway, or energy metabolism, thus establishing an optimal microenvironment that facilitates tissue regeneration [16]. Despite the fact that BOICs have shown excellent results in tissue regeneration engineering, little is known about the fundamental laws and underlying mechanisms by which the physicochemical properties of BOICs regulate cell behavior and the biological microenvironment. Hence, there are still some challenges in fabricating and developing BOICs that have suitable mechanical properties and biocompatibility. Furthermore, the complexity of manufacturing processes and concerns about the long-term biological safety and stability of bioinspired materials restrict the translation of BOICs into clinical use. Conquering these challenges and addressing these requirements are essential for the advancement of BOICs in tissue regeneration engineering.

This review presents an overview of the concepts and recent advances in the biologically inspired construction of multifunctional BOICs utilizing artificial techniques, as well as for applications in tissue regeneration engineering (Fig. 1). Firstly, a brief section summarizes two typical biominerals with hierarchically ordered structures (bones and teeth), the relationship between the structure and composition, and the specific properties. Secondly, a detailed description is given of constituent materials and various approaches for constructing BOICs. Meanwhile, the applications of BOICs in tissue regeneration engineering were summarized in this article. Finally, a detailed discussion is presented about the key lessons offered by BOICs preparation in attempts to implement them in practical synthetic structures. The challenges and development prospects presented provide additional insight into the future development of BOICs, as well as expanding their applications in tissue regeneration engineering.

## 2 Hierarchically ordered structures and mechanical properties of natural bones and teeth

The biomineralization process brings inorganic minerals into the organism, generating a wide range of biominerals with delicate hierarchically ordered structures and excellent mechanical properties, which are represented and optimized at each level [17]. Thus, accurately simulating the hierarchical structures of biominerals and preparing BOICs with excellent properties are mainstream in the biomineralization field. Next, we will elaborate on biominerals with typical hierarchically ordered structures and superior mechanical properties, namely bones and teeth.

### 2.1 Natural bones

Bones are naturally occurring organic–inorganic composites that serve as the structural materials for the internal scaffolding of vertebrates [18]. Bone has a highly hierarchical structure, mainly composed of mineralized collagen fibril bundles, with 65% inorganic substances (mainly HAP) and 25% organic substances (mainly type I collagen fibrils). The precise organization of collagen fibrils and HAP nanocrystals at the nanoscale brings about nanomechanical heterogeneity, enabling high energy dissipation and resistance to fracture. Collagen is responsible for shear modulus and breaking strength, whereas HAP endows bone with marvelous tensile modulus and hardness. The physiological functions and mechanical properties of bones depend on their special hierarchically ordered structures [19]. In the bone formation process, osteoblasts enrich calcium and phosphorus ions in the organic matrix to generate amorphous calcium phosphate (ACP) nanoclusters, and then ACP infiltrates into collagen fibrils and crystallizes to generate small-sized (about 1.5–4 nm thick,

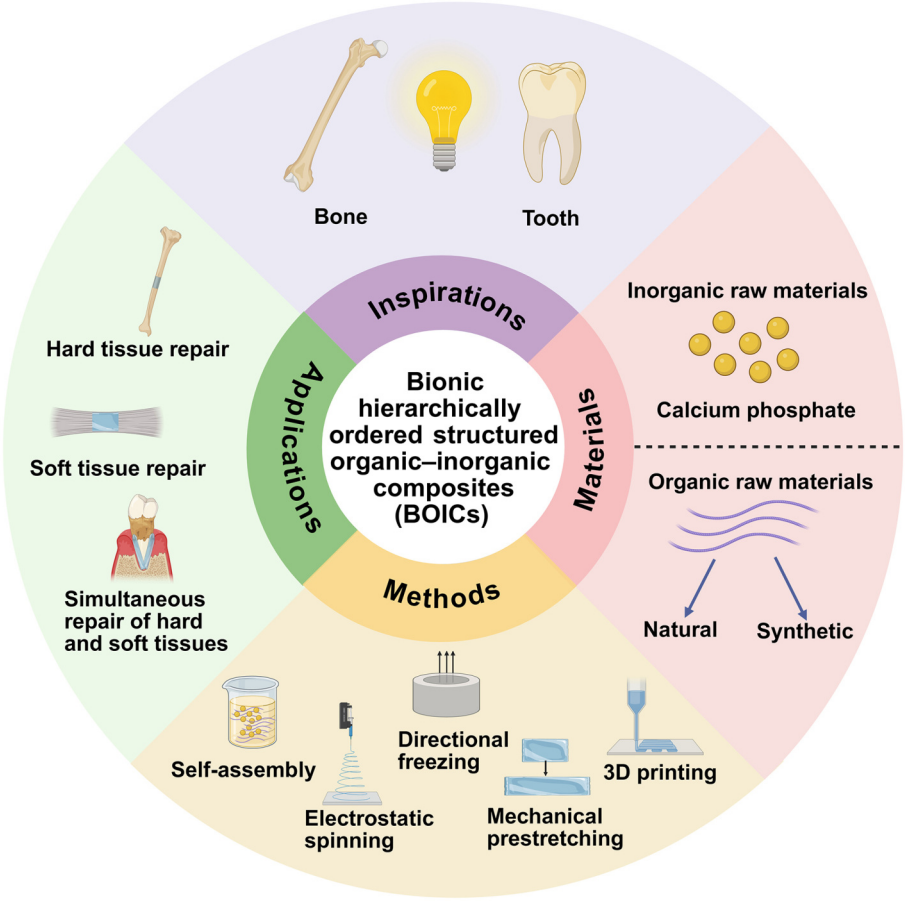


**Figure 1** Overview of the constituent materials and design strategies for fabricating the bioinspired BOICs and their applications in tissue regeneration engineering.

20–50 nm long) HAP with hexagonal crystal structure, which ultimately generates bones with special hierarchically ordered structures and superior functions [20]. Nair et al. classified bones into six levels. The hierarchically ordered structures of bones provide various interfaces from the microscopic to the macroscopic level, following the order: nanophases (collagen molecules and mineral particles), mineralized fibril (~ 100 nm), fiber bundle (~ 0.5 μm), lamella (~ 5 μm), and osteon (~ 10–500 μm) (Fig. 2(a)) [21]. Furthermore, Weiner et al. classified the bone into seven structural layers and divided the overall bone into cortical and cancellous bone, with a dense outer layer of cortical bone encircling an inner, highly porous marrow cavity formed by trabecular or cancellous bone (Fig. 2(b)) [22]. These micro- and nanoscale hierarchically ordered structures provide bones with high Young's modulus (10–20 GPa) and strong toughness (2–7 $kJ \cdot m^{-2}$) (Fig. 2(c)) [23]. Meanwhile, the chemical composition and hierarchical structures of natural bones have potential inspirations for designing and synthesizing biomimetic materials with optimized functions, which can effectively integrate with human tissues and enhance bone regeneration and repair.

### 2.2 Natural teeth

Teeth are also typical organic–inorganic composites, primarily composed of enamel and dentin. Tooth enamel is a highly ordered prismatic structure of HAP, consisting of approximately 96% inorganic material and only 1% organic substances (mainly amelogenins) [24]. Due to its extremely high mineral content, enamel is a very fragile tissue. Dentin is the main body of teeth and has a more complex structure that protects the pulp and supports the overlying enamel. Dentin has a similar composition to that of bone. The collagen structure of dentin is complex, with collagen oriented in a helical structure forming tubules, but transforming to radial in the plane perpendicular to the direction of the tubules (Fig. 2(d)) [25]. Dentin has a two-layered structure, where hard peritubular dentin containing dentin tubules is embedded in soft intertubular dentin (Fig. 2(e)) [26]. Peritubular dentin is composed of carbonate apatite and a very small amount of organic matrix, whereas intertubular dentin is rich in reticulated mineralized collagen fibrils, which are structurally similar to bone mineralized collagen fibrils. Noncollagenous proteins and proteoglycans (e.g., acidic glycosaminoglycans) act as gluing molecules to hold the mineralized collagen nanofibrils together and provide a mechanism for energy dissipation in dentin. The mechanical properties of dentin vary depending on the mineral content, with highly mineralized peritubular dentin having a Young's modulus of 40–42 GPa, while weakly mineralized intertubular dentin has a Young's modulus of 17 GPa [27]. Dentin also has an excellent flexural modulus, which decreases with an increase in tubule density, ranging from approximately 15–20 GPa (Fig. 2(f)) [28]. The hierarchically ordered structure of dentin gives it sufficient elasticity and strength to enable teeth to withstand immense mechanical loads during gnawing and chewing. This property has also become a primary focus of numerous bionic investigations.

## 3 Constituent materials with BOICs

Recently, the development of BOICs has drawn inspiration from

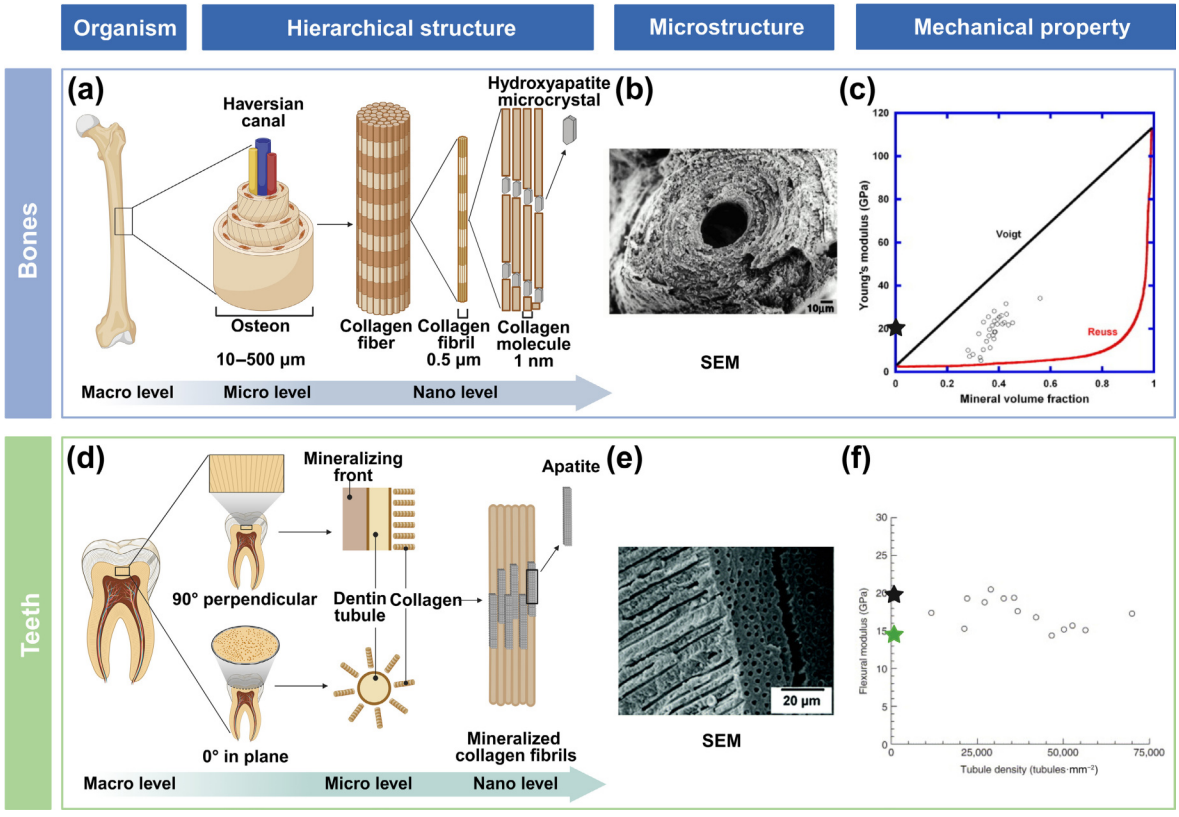


**Figure 2** Hierarchically ordered structures and mechanical properties of typical biominerals, namely bones and teeth. (a) Schematic illustration of the hierarchically ordered structure of natural bones from the macro scale to the nano scale. (b) Scanning electron microscopy (SEM) image of a single osteon from human bone. Reproduced with permission from Ref. [22], © TMS 2013. (c) Effect of mineral volume fraction on the mechanical properties of bones. Reproduced with permission from Ref. [23], © Elsevier Ltd. 2007. (d) Schematic illustration of the hierarchically ordered structure of natural teeth from the macro scale to the nano scale. (e) SEM image of dentinal tubules. Reproduced with permission from Ref. [26], © Royal Society of Chemistry 2016. (f) Effect of tubule densities on the mechanical properties of teeth. Reproduced with permission from Ref. [28], © Elsevier Ltd. 2005.

the hierarchically ordered structures found in organisms and has garnered substantial interest from scientists. It is well known that the biocompatibility and mechanical properties of BOICs are largely influenced by their constituent materials. This section will provide a brief overview of the composition materials. To classify the constituent materials used in fabricating BOICs, we categorize them into inorganic and organic raw materials. For inorganic materials, calcium phosphate (CaP), as the main inorganic component in fabricating BOICs, will be discussed. For organic materials, we further categorize them into natural polymers and synthetic polymers. Generally, the synthesis ratio between organic and inorganic raw materials within BOICs is also a crucial factor influencing their mechanical strength, bioactivity, and degradation behavior [29]. Overall, the optimal ratio depends on the specific application requirements and the chosen fabrication method, which together determine the hierarchical structure and interfacial compatibility of the resulting BOICs [30, 31]. Table 1 presents a comprehensive overview of the compositional materials and their organic/inorganic mass ratio (w/w), bioinspired organisms, fabrication methods employed in constructing BOICs, and tissue regeneration engineering applications as documented in the literature.

### 3.1 Inorganic raw materials-CaP

CaP is the main inorganic component of vertebrate bones and teeth with good biocompatibility, attracting particular attention from the scientific community focused on bone regeneration [32]. The commonly utilized forms of CaP include HAP, dicalcium phosphate, octacalcium phosphate, dicalcium phosphate dihydrate, and ACP, which represents a precursor stage of bone formation [31]. Among them, HAP is the main inorganic component in the endoskeletons of many organisms. Jarcho M. independently synthesized HAP, which began to be widely used in bone repair surgery as a substitute material, marking one of the earliest applications of bioactive ceramics in orthopedics [33]. However, since HAP materials have poor mechanical properties, high brittleness, and weak osteoconductivity, researchers have continued to optimize the materials by adding organics such as collagen, cellulose, and alginate [34, 35]. Furthermore, organic–inorganic composites for tissue regeneration engineering applications require precise control of the material composition and structure, as well as the size of the particles, since pore size and interconnectivity affect the regeneration process. Stoehr et al. found that needle-like CaP particles do more damage to cells than spherical particles [36]. In addition, HAP surfaces with hierarchically ordered structures showed high performance in protein adsorption, cell adhesion, osteogenic differentiation, and angiogenesis-related gene expression [37]. Abels et al. demonstrated that synthetic HAP particles within the size of 0.5–2 mm elicited the lowest inflammatory response *in vivo* compared to smaller ones [38]. Thus, optimization of the properties (such as size and morphology) of CaP particles can lead to BOICs with improved properties.

In recent years, NCaPs with different sizes and morphologies

**Table 1** BOICs prepared from natural and synthetic polymers and their applications (n-HAP, nano-hydroxyapatite)

| Categories of composites | Prepared BOICs | Organic/inorganic mass ratio (w/w) | Bionic structures | Preparation methods | Applications | Refs. |
|---|---|---|---|---|---|---|
| Natural polymers | Collagen/HAP | 7:13 | Bionic bone | 3D printing | Bone repair | [85] |
| | Cellulose/HAP | 3:7 | Bionic bone and tooth | Mechanical prestretching | Hard tissue repair | [86] |
| | Amyloid fibrils/HAP | 2:3 | Bionic bone | Filtration-induced organization | Bone repair | [87] |
| | Alginate/HAP | 40:1 | Bionic bone | Spin-coating/brushing-assembly | Bone repair | [88] |
| | BC/HAP | 1:9 | Bionic bone | Mechanical prestretching | Bone substitutes | [89] |
| | CS/HAP | 1:2 | Bionic bone | Directional freezing | Bone repair | [90] |
| | SF/HAP | — | Bionic bone | 3D printing | Bone repair | [91] |
| | Collagen/ACP | 1.2:1 | Bionic bone | Bioskiving | Bone repair | [92] |
| | CS/gelatin/HAP | 7:3 | Bionic narce | Directional freezing | Bone repair | [93] |
| | Gelatin/HA/HAP | 5:1 | Bionic bone | 3D printing | Bone repair | [94] |
| | PCL/HAP | — | Bionic osteochondral | 3D printing | Osteochondral repair | [95] |
| | PVA/PAA/CaP | — | Bionic tooth | Directional freezing | Tooth repair | [96] |
| | PLA/HAP | 7:3 | Bionic bone | 3D printing | Bone repair | [97] |
| | PEKK/n-HAP | — | Bionic bone | Self-assembly | Bone repair | [98] |
| Synthetic polymers | Hyaluronic acid methacrylate/ HAP | 1:4 | Bionic bone | 3D printing | Bone repair | [99] |
| | GelMA/methacrylic anhydride silk fibroin/HAP | 7:1 | Bionic bone | 3D printing | Bone repair | [100] |
| | GelMA/alginate methacrylate/HAP | 26:1 | Bionic bone | 3D printing | Bone repair and organoid formation | [101] |
| | Piezoelectric polymer poly-L-lactic acid/HAP | — | Bionic bone | Piezoelectricity | Bone repair | [102] |
| | Poly(γ-benzyl-L-glutamate)/n-HAP | 5:3 | Bionic bone | 3D printing | Bone repair | [103] |
| | Collagen/PCL/n-HAP | 2:1 | Bionic periosteum | Self-assembly | Bone repair | [104] |
| Natural and synthetic polymers | Gelatin/CS/PVA/ n-HAP | 7:1 | Bionic bone | Directional freezing | Bone repair | [105] |
| | PLA/polydopamine/ sodium alginate/ carboxymethyl chitosan/n-HAP | — | Bionic bone | 3D printing | Bone repair | [106] |

have been synthesized and stabilized by various biomolecules, such as nucleic acids and polymers. Capitalizing on the unique properties of RNA, an RNA-ACP with an average hydrodynamic diameter of 99.42 nm has been developed (Figs. 3(a) and 3(b)) [39]. In addition, polyethylene glycol-inositol 1,3,4,5,6-pentakisphosphate stabilized NCaPs (diameter ~ 40 nm) were prepared and can quickly turn into needle bundle-like crystals with a size of about 80 nm in a few hours (Figs. 3(c) and 3(d)) [40]. Moreover, CaP complexes stabilized by poly (allylamine hydrochloride) (PAH) were fabricated, with an average hydrodynamic diameter of 17.9 nm (Figs. 3(e) and 3(f)) [41]. The previous size of the synthetic CaP was generally above 20 nm, and the resulting organic–inorganic composites had significant phase separation, which greatly limited the performance of the prepared composites. Researchers have achieved improvements in the mechanical properties of composites by further reducing the size of the inorganic units and increasing their dispersion within the organic matrix. In 2019, Tang's group fabricated a novel type of removable small organic molecule, namely triethylamine-stabilized calcium phosphate ion clusters (CPICs), with an average diameter of 1.5 ± 0.3 nm (Figs. 3(g) and 3(h)) [5]. The prepared CPICs can establish a bionic crystalline-amorphous mineralization frontier to induce the epitaxial growth of enamel with the integrity of the enamel mineral phase. Furthermore, they took a unique approach to polymerization and cross-linking of inorganic ionic compounds by using organic monomers as precursors through covalent bonding [42]. That is, when the polymerization and cross-linking of organic and inorganic materials occur simultaneously, the two can be homogeneously compounded and the interfacial phase eliminated, thus achieving polymerization on a molecular scale and preparing novel organic–inorganic copolymer materials with high optical transparency, excellent mechanical properties, and superior stability [43]. Additionally, integration of inorganic HAP with the organic monomer polyvinyl alcohol (PVA) can prepare spider silk-like hybrid fibers with a hierarchical structure and exceptional toughness (296 ± 12 $J \cdot g^{-1}$) [44].

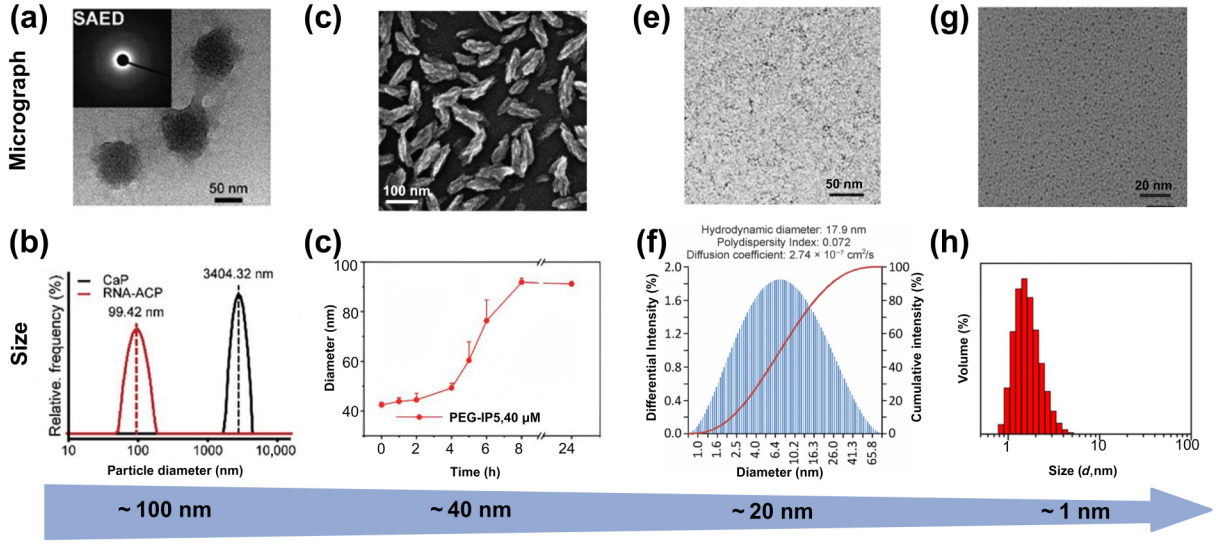


**Figure 3** NCaPs of different particle sizes. (a) High-resolution transmission electron microscopy image of the prepared RNA-ACP and (b) the size distribution of RNA-ACP (red line) as determined by dynamic light scattering (DLS). The inset shows the selected area electron diffraction pattern of RNA-ACP. Reproduced with permission from Ref. [39], © Wiley-VCH GmbH 2024. (c) SEM image of the prepared CaP nanoparticles and (d) the size distribution of CaP nanoparticles as determined by DLS. Reproduced with permission from Ref. [40], © American Chemical Society 2017. (e) Transmission electron microscopy (TEM) image of the PAH-stabilised CaP solution and (f) the size distribution of PAH-stabilised CaP nanoparticles as determined by DLS. Reproduced with permission from Ref. [41], © Springer Nature Limited 2016. (g) TEM image of the prepared CPICs and (h) the size distribution of CPICs as determined by DLS. Reproduced with permission from Ref. [5], © Shao, C. Y. et al., some rights reserved; exclusive licensee American Association for the Advancement of Science 2019.

## 3.2 Organic raw materials

### *3.2.1 Natural polymers*

Various natural polymers with multifunctionality, excellent biocompatibility, and biodegradability are involved in the formation of BOICs, such as collagen, alginate, cellulose, hyaluronic acid (HA), chitosan (CS), and silk fibroin (SF). Collagen is the most abundant protein in mammals and a major component of the ECM. Among these, type I collagen, with a diameter of 80–100 nm, is the most important component of the organic phase in bone [45]. Collagen has sites on its surface that promote osteoblast attachment and mineral deposition, and a large body of evidence has demonstrated the positive role of collagen in hard tissue mineralization to date [46]. It can not only control the penetration of ACP into collagen and induce HAP nucleation, but also control the transformation of a crystal nucleus into a crystalline phase. Alginate is an acidic straight-chain and water-soluble polysaccharide, and is also the most abundant biopolymer in the world [47]. It consists of 1,4-linked β-D-mannuronic acid (M) and 1,4 α-L-guluronic acid (G) residues, with only the carboxylate group of the G residue capable of cross-linking with divalent cations such as calcium ion ($Ca^{2+}$) to form composites. Accordingly, alginates with a high G content form stiffer composites, whereas those with a high M content produce softer elastic ones. Its mucosal adhesion properties also extend its use in applications such as drug delivery [48]. Cellulose, which is composed of hundreds to millions of glucose units connected with β-1,4-glycosidic bonds, is also a good choice for future materials [49]. Moreover, due to its hierarchically ordered anisotropic structures, cellulose nanofiber is an ideal candidate for guiding bionic mineralization with OH groups to form strong hydrogen bonds with various molecules. Among these, bacterial cellulose (BC) with superior mechanical properties (Young's modulus is 20 GPa for sheets and 130 GPa for single fibers) and chemical properties, is frequently employed to synthesize BOICs for tissue regeneration engineering [50, 51]. HA is a naturally occurring polysaccharide that is one of the main components of the ECM of skin and cartilage [52]. The large number of carboxyl and hydroxyl groups present in HA gives it a highly hydrophilic character. Thus, it plays a vital role in various cell biological behaviors such as migration, proliferation, and differentiation [53]. Moreover, HA also has good gel-forming properties and an easy-to-modify chemical structure that promotes the biomineralization of CaP, which has great potential in tissue regeneration engineering [54]. CS is a natural linear polysaccharide and the second most abundant natural polymer [55]. It is non-toxic, antibacterial, hemostatic, and has excellent mechanical properties [56]. The properties of CS are mainly affected by the degree of deacetylation and molecular weight; CS with higher deacetylation and molecular weight is more attractive for tissue regeneration engineering applications [57]. Furthermore, the structure of CS is highly similar to glycosaminoglycans in the human body, which is perfectly compatible with the alkaline internal environment of the organism and is used as a bone scaffold for cell attachment and proliferation in bone defect repair [58]. SF is a naturally occurring protein-based biopolymer with tunable mechanical properties and low inflammation to host tissues. SF has various secondary structures, including α-helix, β-sheet, and crossed β-sheet. The high content of the β-folding structure gives it good mechanical strength and resilience; the unique arginine-glycine-aspartate sequence in the molecule promotes cell adhesion and regulates cell behavior; the active amino acid side chains can provide attachment sites for other compounds [59]. However, natural polymers usually exhibit poor mechanical properties and inadequate cellular interactions, limiting their direct applications in tissue regeneration engineering. Integrating them with inorganic minerals like CaP via bionic mineralization is a promising strategy to achieve materials with better mechanical properties, which is of great significance for tissue regeneration engineering [60, 61].

#### 3.2.2 *Synthetic polymers*

In contrast to natural polymers, synthetic polymers often exhibit superior and adjustable mechanical properties, such as polycaprolactone (PCL), PVA, polylactic acid (PLA), polyacrylic acid (PAA), and polyaryletherketones (PAEK), are also frequently used for preparing BOICs. PCL is an aliphatic polyester obtained by ring-opening polymerization of ε-caprolactone. It has favorable characteristics such as strong hydrophobicity, semicrystallinity, and a low melting point, which makes it widely used in tissue regeneration engineering [62]. PVA with non-toxicity, water solubility, and blood compatibility, is one of the most commonly used synthetic polymers [63]. It can form polymeric networks through freezing-thawing cycles that serve as scaffolds for tissue regeneration engineering [64]. PLA is an aliphatic polyester obtained from lactic acid [65]. It has high tensile strength and has been widely researched in tissue regeneration engineering, such as vascular stents and bone fixation. After implantation as bone substitute materials, it can be naturally hydrolyzed into lactic acid and converted into water and carbon dioxide, eventually discharged from the body, thus causing no significant harm to the human body. PAA is a water-soluble polymer synthesized by polymerizing acrylic acid monomers in an aqueous solution using persulfate as an initiator [66]. PAA has good capacity for dry adhesion and hemostasis; thus, it has been widely applied in commercial wound dressings [67]. Moreover, due to the presence of carboxyl groups, pH-responsive nanogels can be prepared by chelating with metal ions and adhering to bone tissue through chemical bonding and non-covalent interactions [68]. PAEK are a class of ultra-high-performance polymers consisting of a class of phenylene rings linked by an oxygen bridge (ether bond) and a carbonyl group (ketone). PAEK has excellent temperature and chemical resistance, as well as excellent fluid stability. According to the molecular chain in the ether bond, ketone group, and benzene ring connection order and proportion of different types, it can form many other polymers, such as polyether ether ketone, polyether ketone, and polyether ketone cross polymer (PEKK) [69]. Nevertheless, synthetic polymers also face several challenges, including poor biocompatibility and degradation. Combining them with inorganic materials, such as CaP, to form BOICs can effectively improve bioactivity, the degradation performance, and mechanical properties [70, 71]. In addition to conventional synthetic polymers, multifunctional polyurethane (PU) has recently exemplified significant progress in tissue regeneration engineering [72]. Owing to its controllable biodegradability, excellent biocompatibility, highly tunable chemical composition, and mechanical properties, PU can be rationally engineered to match the mechanical requirements of both soft and hard tissues. Moreover, by integrating with inorganic materials such as CaP, it can further enhance osteogenic bioactivity while maintaining favorable mechanical resilience and processability, making it a viable candidate for developing next-generation BOICs [73].

#### 3.2.3 *Ideal organic matrices: Integration of natural and synthetic polymers*

While natural and synthetic polymers each offer distinct advantages for constructing BOICs, they also present inherent limitations, as previously discussed. To address these challenges and pursue ideal organic matrices that simultaneously fulfill biological and mechanical requirements, researchers have focused on the development of composite polymers [74, 75]. The construction strategies of composite polymers are diverse, including physical blends, chemical conjugations, or the formation of interpenetrating networks. For instance, collagen or CS, which provide cell recognition sites and enhance bioactivity, can be blended or cross-linked with synthetic polymers like PCL or PAA [76–78]. This integration can improve the otherwise weak mechanical strength and rapid degradation rate of the natural polymer, while endowing the synthetic polymer with better cell adhesion and tissue integration capabilities. Similarly, HA has been incorporated into PVA networks to create hydrogels that not only possess the desirable swelling and biocompatibility of HA but also exhibit enhanced mechanical properties due to PVA [79]. Other natural polymers with excellent biocompatibility, such as SF and BC, can also be combined with various synthetic polymers to enhance toughness, catering to complex tissue regeneration needs [80–82]. In the construction of BOICs, these composite polymers serve as sophisticated organic raw materials for the bionic mineralization of inorganic phases, notably CaP. The natural polymers can actively guide and nucleate the growth of HAP nanocrystals, whereas the synthetic polymers ensure the composites maintain structural integrity throughout the mineralization process and subsequent applications [83]. The integration of natural and synthetic polymers is particularly promising for tissue regeneration engineering, as it moves beyond the limitations of single-component materials toward truly biomimetic and multifunctional materials. Therefore, the exploration of natural and synthetic polymer composites represents a pivotal direction in advancing the organic constituents of BOICs, holding great potential for developing next-generation biomaterials that more closely replicate the complex interplay of biological functions and mechanical resilience in biominerals [84].

## 4 Fabrication strategies of BOICs

BOICs require not only optimized constituent materials but also auxiliary structural engineering strategies to effectively mimic the hierarchically ordered structures and multifunctional characteristics of biominerals [107]. In recent years, diverse structural engineering approaches have been developed for fabricating BOICs with controlled microarchitectures [108]. This section briefly reviews key fabrication methodologies, including self-assembly, electrospinning, directional freezing, mechanical prestretching, and 3D printing. Table 2 summarizes their advantages and disadvantages, respectively. These advanced fabrication strategies provide versatile foundations for developing next-generation BOICs with tailored structure-property relationships.

### 4.1 Self-assembly

Self-assembly is a method in which molecular units or nanoparticles are spontaneously organized into sequential structures by non-covalent interactions [109]. It emphasizes the spontaneity and reversibility of the inter-component interactions, which is carried out under mild conditions [110]. By using acrylamide and CPO as raw materials, a robust, lightweight, and thermal insulating composite with a hierarchically ordered structure was synthesized through self-assembly (Fig. 4(a)) [111]. Recently, a composite named "osteomimix" was also prepared by self-assembly using sodium methacrylate-carboxymethyl cellulose-stabilized amorphous magnesium calcium phosphate and methacrylate-modified type I collagen as raw materials [112]. The prepared osteomimix had an optimal bionic microenvironment

**Table 2** Comparisons of the commonly used fabrication strategies. Summarized from Refs. [109–141]

| Fabrication strategies | Advantages | Disadvantages |
|---|---|---|
| Self-assembly | -Spontaneous organization under mild conditions<br>-High structural precision and controllability<br>-Suitable for creating hierarchically ordered bionic structures | -Structural defects and residual impurities are difficult to avoid<br>-Limited mechanical strength for load-bearing applications<br>-Requiring further validation for broad applicability |
| Electrostatic spinning | -Preparing ECM-mimicking nanofibers with high specific surface area, semi-permeability, and promotion of cell adhesion<br>-Versatile material compatibility<br>-Enabling fabrication of hierarchically ordered fibrous structures | -High process complexity<br>-Fiber size strongly depends on material itself (e.g., molecular weight, molecular weight distribution, and solubility) and solution properties (e.g., viscoelasticity, concentration, and surface tension)<br>-Sensitive to electric field strength and equipment geometry |
| Directional freezing | -Mild and controllable processing conditions<br>-Versatile for anisotropic porous and lamellar structures<br>-Bidirectional freezing enables enhanced structural control for complex, hierarchically ordered structures with improved properties | -Unidirectional freezing has limited structural complexity<br>-Bidirectional freezing requires complex equipment and precise control<br>-Mechanical properties are highly process-dependent |
| Mechanical prestretching | -High structural controllability along the stretching direction<br>-Exceptional tensile strength and toughness<br>-Great structural similarity to soft tissues<br>-Efficient for fabricating anisotropic, high-strength hydrogels | -Limited to viscoelastic materials<br>-Limited shape complexity<br>-Sensitive to the degree of prestretching and moisture control. |
| 3D printing | -High structural complexity and design flexibility<br>-Enabling multi-material, multi-scale, and multi-functional fabrication<br>-Suitable for customized scaffolds | -Limited by the properties of biomaterial inks (e.g., viscosity, rheology, post-printing stability)<br>-Potential cytotoxicity from some ink components (e.g., photoinitiators in GelMA)<br>-Limited printing resolution, sample size, and productivity |

and hierarchically ordered structure, and could be customized for the repair of irregular bone defects using computer-aided design/computer-aided manufacturing (CAD/CAM) technology.

Self-assembly is a promising fabrication strategy due to its precise controllability and intrinsic ability to integrate hybrid materials [113, 114]. Nevertheless, it faces critical challenges in minimizing structural defects and residual impurities, especially when designing mechanically demanding, hierarchically ordered architectures. It requires systematic validation in a variety of biological systems and functional prototypes to determine its versatility in creating hierarchically ordered bionic structures.

### 4.2 Electrostatic spinning

Electrostatic spinning transforms solutions or melts (mainly polymers) into continuous fibers with a micrometer to a nanometer in diameter, utilizing high-voltage direct current electricity, similar to collagen fibers in the ECM [115]. It can be applied to synthetic and natural polymers, nanoparticle polymers, etc. The produced fibers have a wide range of structures, from single fibers to ordered arrangements of fibers, porous structures, and high specific surface areas [116]. In addition, it allows the immobilization of non-fiber forming substances such as zwitterions and inorganic metal salts, and the preparation of BOICs. The DNA-HAP ordered composite prepared by electrostatic spinning exhibits an ultrahigh Young's modulus of ~ 25 GPa, which is comparable to natural HAP and surpasses that of most artificial mineralized composites (Fig. 4(b)) [117]. Moreover, it was shown that the electrostatically spun composites prepared based on PCL and HAP have good biocompatibility, and 3D scaffolds made from the composites enhance osteoblast attachment and proliferation, making them ideal for bone regeneration and dental implants [118].

Electrostatic spinning allows the controlled synthesis of composites with high specific surface area, semi-permeability, and promotion of cell adhesion [119]. However, it has a high degree of complexity, and the size of the fibers formed is influenced by the properties of the polymer itself (e.g., molecular weight, molecular weight distribution, and solubility) as well as the properties of the polymer solution (e.g., viscoelasticity, concentration, and surface tension). Moreover, the strength of the electric field and the geometry also play a major role in fiber formation.

### 4.3 Directional freezing

Directional freezing is carried out under very mild conditions to produce a solid material by non-destructively removing the ice template by freeze drying and sublimation [120, 121]. It can precisely control the structure of the synthetic materials by changing the freezing temperature and the freezing rate. In the classical unidirectional freezing process, a steep temperature gradient is imposed by cooling from a single direction, leading to pore channels and lamellar structures aligned along one dominant orientation [122]. While this approach is effective for generating anisotropic porous architectures, its structural complexity is inherently limited, making it difficult to replicate the hierarchically ordered structures commonly found in biomaterials. To address these limitations, bidirectional freezing has been developed, in which temperature gradients are simultaneously applied along two orthogonal directions [123]. This configuration is achieved by designing molds and cooling devices that allow two independently controlled cold sources to create perpendicular temperature fields. The interaction of these two temperature gradients induces complex ice crystal growth, guiding the formation of interconnected lamellar or channeled porous structures with multiscale hierarchical ordering. Compared with unidirectional freezing, it allows enhanced structural control and greater design flexibility, enabling the fabrication of hierarchically ordered structured materials with improved mechanical properties and biological functionality. For instance, a hierarchically ordered structured composite has been successfully prepared, incorporating CS and HAP nanoparticles, demonstrating excellent biocompatibility and bioactivity, and can be used for bone regeneration [90]. What's more, by using PVA and HAP as raw materials, an enamel analog with a hierarchically ordered structure was engineered through bidirectional freezing (Fig. 4(c)) [124]. The prepared composite exhibited high stiffness, hardness, strength,

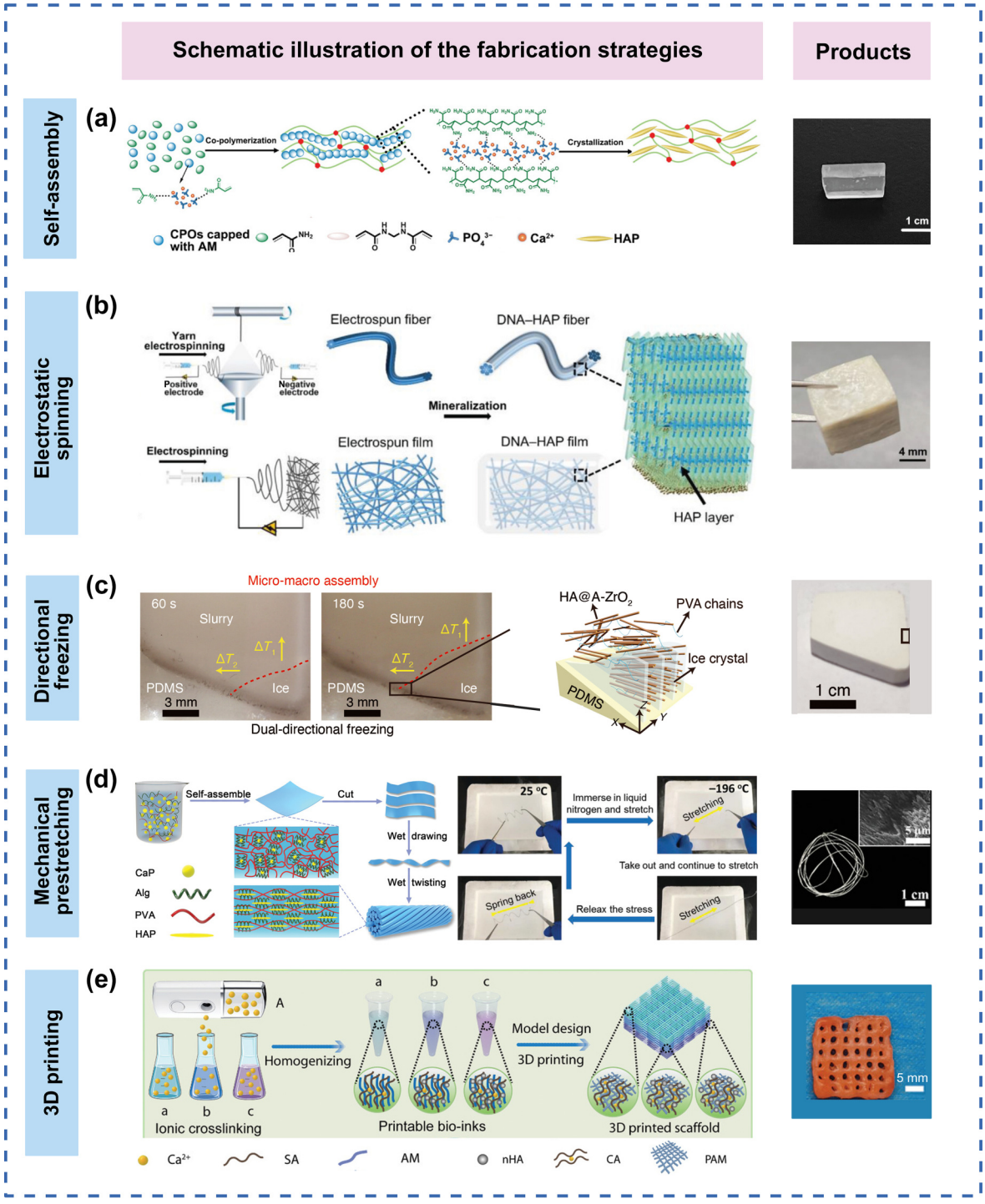


**Figure 4** Typical conventional fabrication strategies of BOICs. (a) Schematic illustration of the fabrication route of self-assembly and the photograph of the product. Reproduced with permission from Ref. [111], © Wiley-VCH GmbH 2024. (b) Schematic illustration of the fabrication route of electrostatic spinning and the photograph of the product. Reproduced with permission from ref. [117], © Wiley-VCH GmbH 2022. (c) Schematic illustration of the fabrication route of directional freezing and the photograph of the product. Reproduced with permission from Ref. [124], © Zhao, H. W. et al., some rights reserved; exclusive licensee American Association for the Advancement of Science 2022. (d) Schematic illustration of the fabrication route of mechanical prestretching and the photograph of the product. Reproduced with permission from Ref. [44], © WILEY-VCH Verlag GmbH & Co. KGaA, Weinheim 2019. (e) Schematic illustration of the fabrication route of 3D printing and the photograph of the product. Reproduced with permission from Ref. [135], © Wiley-VCH GmbH 2020.

viscoelasticity, and toughness, surpassing the properties of enamel and previously prepared bioinspired materials. Despite these advantages, bidirectional freezing presents greater technological challenges than unidirectional freezing [125]. It requires precise coordination between multiple cooling sources, accurate synchronization of temperature gradients and freezing rates, and meticulous control over the interaction dynamics of ice crystal growth to ensure reproducibility. The equipment and mold design are also significantly more complex than unidirectional freezing, increasing both cost and operational difficulty.

Overall, directional freezing is a controllable and versatile method for manufacturing hierarchically ordered structured lamellar and porous materials [126]. Nevertheless, further improvement of the mechanical properties of the bionic structures remains challenging, with freezing temperature, sintering additive content, and sintering temperature all influencing the microstructure and compressive strength of the prepared materials.

### 4.4 Mechanical prestretching

Mechanical prestretching is an efficient strategy for preparing anisotropic, ultrastrong hydrogels, which have great structural similarities with the soft tissues of living organisms [127, 128]. It involves repeatedly training the randomly distributed hydrogel network structure to arrange in a hierarchically ordered structure along the stress direction. The prepared hydrogels have pronounced anisotropic properties, including oriented molecular fiber bundles and extended grain sizes, which give the materials a full range of mechanical properties [129]. Based on this, spider silk fibers-like macrofibers with a hierarchically ordered structure were designed by using HAP and PVA as raw materials (Fig. 4(d)) [44]. The prepared macrofibers exhibited a exceptionally high tensile strength of 949 ± 38 MPa, a specific toughness of 296 ± 12 $J \cdot g^{-1}$, and a stretchability of 80.6%, which are superior to most synthetic fibers, and thus can be used as potential bioinspired materials in tissue regeneration engineering, such as ligaments and tendons.

Mechanical prestretching is an effective method to construct anisotropic hydrogels with excellent mechanical properties and biocompatibility. Nevertheless, different degrees of prestretching and moisture control affect the mechanical properties of the composites; thus prestretching and moisture need to be controlled to improve the strength of the bioinspired materials.

### 4.5 3D printing

3D printing is a powerful manufacturing technique to build complex 3D architectures that mimic the hierarchically ordered structures of natural tissues, such as replicating primitive tissues and organs or providing appropriate cell-material interfaces [130]. It prepares bioinspired materials with multi-scale, multi-material, and multi-functionality by stacking the biomaterial inks layer by layer under the precise control of the composition and spatial distribution of cells and composites. Biomaterial inks, typically composed of polymer matrices (e.g., collagen, alginate, HA, GelMA), crosslinking agents, and cellular components, must exhibit specific physical properties such as appropriate viscosity, shear-thinning behavior, and rapid cross-linking capability to ensure printability and structural integrity [131]. Furthermore, the cytocompatibility of these inks is also crucial, thereby enabling support for cell adhesion, proliferation, and differentiation. However, the widely used GelMA presents toxicity concerns due to the photoinitiator, which generates free radicals during light exposure, potentially harming cells. Emerging studies are committed to addressing this issue by involving the use of visible-light photoinitiators, reducing photoinitiator concentrations, and investigating alternative initiator systems like 2,4,6-trimethylbenzoyl-diphenylphosphine oxide nanoparticles or the incorporation of radical scavengers to mitigate oxidative stress [132, 133]. Notably, many biomaterial inks developed from polymers often fail to meet expectations in terms of mechanical strength, scaffold integrity, and the stimulation of tissue formation, thus limiting their applications [134]. Current studies are actively exploring strategies to optimize biomaterial inks, such as the integration of nanoparticles (e.g., nanocellulose, n-HAP) to enhance mechanical properties without compromising biocompatibility. For instance, PLA and n-HAP composite scaffolds were prepared via 3D printing [97]. The printed PLA/n-HAP composite scaffolds have adjustable mechanical strength, and their biocompatibility and osteoinductive properties are better than those of the pure PLA scaffolds, and can be used to repair large bone defects. Moreover, a 3D-printed scaffold was designed with n-HAP gradients similar in structure to osteochondral tissue, exhibiting enhanced mechanical strength, controlled degradation, and superior osteoinductive bioactivity (Fig. 4(e)) [135]. It consists of a cartilage layer (pure hydrogel), an interfacial layer (40/60% (w/w) n-HAP/hydrogel), and a base layer (70/30% (w/w) n-HAP/hydrogel), mimicking the structure of cartilage, calcified cartilage, and subchondral bone, which can significantly enhance cartilage–subchondral bone regeneration.

3D printing, with its high structural complexity and design flexibility, can produce composites with complex 3D shapes that are difficult to obtain by traditional methods [136]. However, it can be limited by the physicochemical properties and cytocompatibility required for biomaterial inks, including viscosity, rheological behavior, and mechanical stability after printing. Inadequate viscosity or poor rheological behavior can lead to nozzle clogging or shape collapse, thus affecting the biological and mechanical properties of the bioinspired materials. Ongoing studies aim to improve biomaterial inks by developing novel ink compositions and incorporating dynamic cross-linking mechanisms to enhance rheological properties, mechanical strength, and biofunctionality [137, 138]. This is exemplified by the design of visible-light-curable HA or GelMA inks [139], n-HAP-enhanced alginate/gelatin inks [140], and dynamic cross-linking HA inks relying on reversible host–guest interactions (β-cyclodextrin/adamantane) [141]. It also faces challenges in terms of sample size, productivity, and achieving nanoscale precision.

## 5 Applications of BOICs in tissue regeneration engineering

In comparison to synthetic materials, biological tissues exhibit superior mechanical properties attributed to their highly organized structural composition. This concept has catalyzed the advancement of BOICs with more delicate structures and superior mechanical strength, which have been accompanied by continuous advances in materials technology. Thus, many high-strength BOICs are poor in biocompatibility owing to the addition of synthetic polymers to improve their mechanical properties, which greatly limit their tissue regeneration engineering applications. As a result, rationally designed BOICs can effectively promote cellular activity and integrate into the *in vivo* microenvironment. In this section, we will focus on various applications of BOICs in tissue regeneration engineering, including hard tissue repair, soft tissue repair, and simultaneous repair of hard and soft tissues.

### 5.1 Hard tissue repair (bone and tooth)

Hard tissue injuries are among the most prevalent human conditions, including bone and tooth injuries [142]. The ability of hard tissues in living organisms to self-repair is limited [143]. Thus, the construction of artificial mineralized materials is important for tissue regeneration engineering applications [144]. However, the mechanical properties of natural mineralized materials are superior to those of synthetic materials. One of the most important problems is the poor interfacial fusion between the restorative

material and the natural tissue, making it difficult to guarantee its mechanical strength. In addition, synthetic bioinspired materials lack bioactivity and degradability in contrast to natural biomaterials. Thus, there is an urgent need to develop novel synthetic materials with both good biocompatibility and excellent mechanical properties by using bionic approaches, which could replicate the structural and functional characteristics of natural hard tissues.

A variety of composites, including titanium alloys, bioceramics, and hydrogels have been developed for bone defect repair. However, most of them are simple structural or non-biological sources that cannot fulfill the requirements of complex bone regeneration. BOICs, which mimic the composition and hierarchically ordered structure of bones, are considered an effective option for developing composites with better bone repair capabilities [145]. Inspired by the development of *in vitro* collagen mineralization, numerous bionic mineralized collagen composites with a bone-like hierarchically ordered structure have been developed to repair bone defects [146]. The high concentration and the ordered arrangement of collagen in BOICs provide an ideal microenvironment for host cell migration and differentiation, and thus have the ability to promote bone regeneration [147]. Other natural organic materials, such as HA, alginate, and CS, as well as synthetic organic materials like PAA, are also frequently combined with CaP to construct BOICs for bone repair [148–150]. Currently, organic polymer/CaP composites have become a research hotspot in bone tissue regeneration engineering, and numerous studies have further shown that biochemical signal propagation and translation play a guiding role in stem cell fate [151]. Mechanistically, stiffness regulates osteogenesis by activating mechanotransduction mediators such as YAP/TAZ and Wnt signaling. Additionally, nanomorphology facilitates osteogenesis by modulating multiple signaling pathways, including the miR-193a-3p-MAP3K3 axis, integrin-mediated focal adhesion formation, HIF-1α signaling, as well as developmental pathways such as Wnt and Hedgehog signaling. Moreover, viscoelasticity regulates osteogenesis by activating mechanotransduction mediators such as HIF-1α and the PI3K/Akt signaling pathways [152]. Importantly, surface curvature of composites also plays a critical role in guiding cellular responses through the activation of mechanosensitive signaling pathways. Studies have shown that surface curvature modulates cell spreading, cytoskeletal tension, and the spatial organization of focal adhesions, thereby activating key signaling pathways such as YAP/TAZ and integrin-mediated FAK signaling, which collectively regulate mesenchymal stem cell migration and differentiation [153, 154]. These curvature-induced signaling pathways are also integrated with biochemical cues, such as IFN-γ/LPS-mediated inflammatory signaling, to synergistically guide osteogenic commitment and bone matrix deposition [155]. Combined with the previous research on bioactive PAEK materials, a porous PEKK scaffold with bone-like apatite coating was designed for spinal repair (Fig. 5(a)) [98, 156, 157]. The results confirmed that the scaffold could mediate osteogenic differentiation of stem cells through activation of the

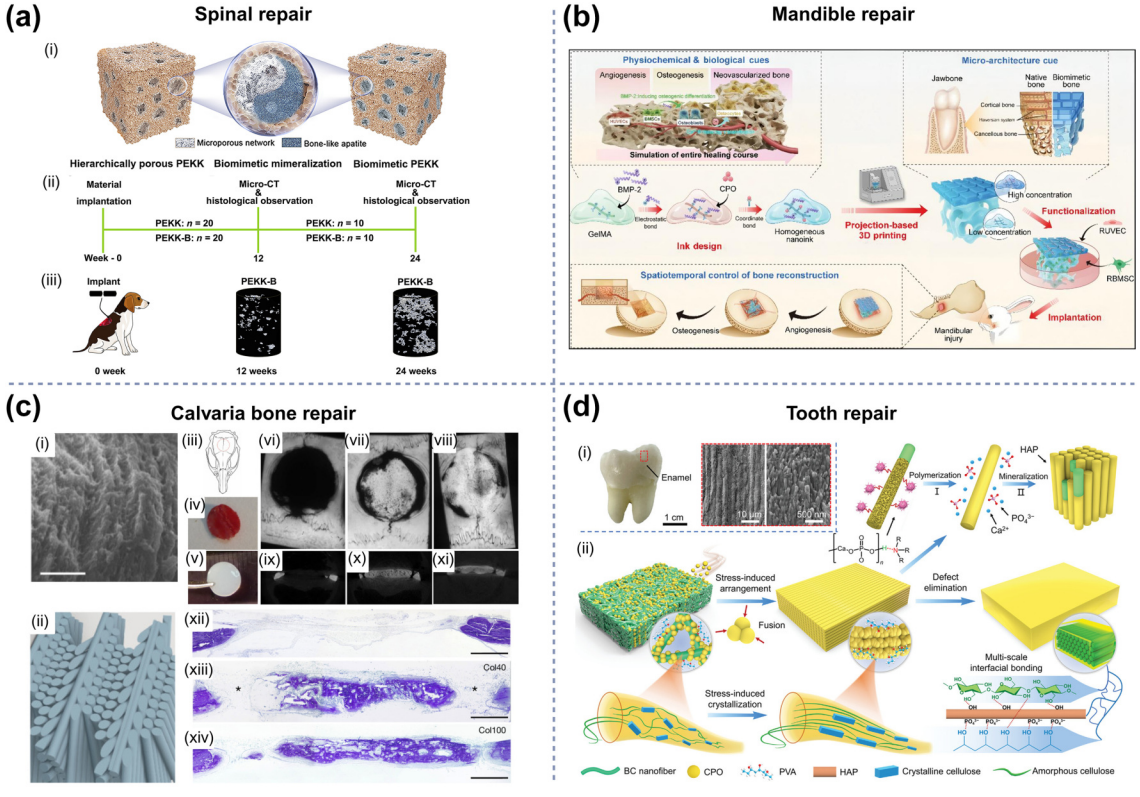


**Figure 5** Functional applications of BOICs in hard tissue repair. (a) Application of BOICs in spinal repair: (i) Schematic illustration of the bionic PEKK scaffold, (ii) *in vivo* experiments, (iii) micro-computed tomography (Micro-CT) evaluation of new bone within the scaffold. Reproduced with permission from Ref. [157], © Yuan, B. et al., some rights reserved; exclusive licensee American Association for the Advancement of Science 2022. (b) Schematic illustration of a hierarchical graft for mandible repair. Reproduced with permission from Ref. [159], © Wiley-VCH GmbH 2023. (c) Application of BOICs in calvaria bone repair: (i) SEM image of synthetic collagen-based materials, (ii) schematic illustration of the plywood organization, (iii)–(v) schematic illustration of the rat calvaria defect model, (vi)–(viii) representative microradiographies, (ix)–(xi) micro-CT scans, and (xii)–(xiv) toluidine-blue-stained histological of control or implanted groups. Reproduced with permission from Ref. [160], © Robin, M. et al. 2024. (d) Application of BOICs in tooth repair: (i) SEM images of tooth enamel, showing an aligned assembly structure and (ii) schematic overview for preparing the bionic organic–inorganic composite. Reproduced with permission from Ref. [163], © Wiley-VCH GmbH 2023.

cAMP/PKA signaling pathway, attributed to the synergistic stimulatory effect of the multistage porous structure and surface bone-like apatite, thereby achieving *in vivo* ectopic induction of new bone formation. This is the first discovery of ectopic induction of osteogenesis in an inert polymer material in more than 50 years, since Winter et al. briefly reported on Poly(hydroxyethyl methacrylate) sponges in *Nature* in 1969 [158]. It has been well-documented that decreasing the size of CaP can effectively produce BOICs with marvelous structures and exceptional mechanical properties. Based on this, our group has successfully prepared CPO (size ~ 1 nm) and intensively explored the use of CPO combined with GelMA to fabricate a hierarchically ordered structured scaffold. By incorporating bone morphogenetic protein (BMP-2) and ultra-small CPO into GelMA precursors, the scaffold for mandible repair, with a cortical layer containing the Haversian system and an interconnected porous cancellous layer, was constructed by 3D printing (Fig. 5(b)) [159]. It exhibits strong osteogenic and angiogenic abilities *in vitro*, which is attributed to the integrin α10/phosphatidylinositol 3 kinase/protein kinase B signaling pathway. More importantly, the newly formed bone with natural tissues induced by this layered grafting facilitates biological function, resulting in a reduction of stresses concentrated around the implant and an expansion of the load-sharing area. This study provides new insights into the development of functionally oriented 3D grafts, which can help BOICs to produce better functional results in bone tissue regeneration engineering. Recently, an innovative 3D mineralized collagen with a "twisted plywood structure" that highly mimics the microscopic structure of natural bone has been developed for calvaria bone repair (Fig. 5(c)) [160]. The high concentration and ordered arrangement of collagens in this mineralized collagen plywood provide an ideal microenvironment for host cell migration and differentiation, ultimately promoting bone maturation and mineralization. The study confirms that the most structurally bionic materials have the potential to stimulate bone growth, highlighting the pivotal role of ECM microstructure in driving cellular behavior in bone.

Restoration of enamel and dentin has also been a difficult challenge in tissue regeneration engineering, as it is often difficult to obtain large restorative layers that are identical to the hierarchically ordered structures of natural teeth and to replicate their properties. The discovery of CaP ion clusters through bionic mineralization strategies has made it possible to achieve tooth remineralization, and organic matrices such as proteins or peptides play an inducing role in the nucleation and growth of CaP minerals, which can be complexed with CaP to obtain tooth-like substances. CaP prenucleating clusters (CaP-PNCs)/starch complexes that enzymatically remove starch and release CaP-PNCs were prepared by mimicking the mechanism by which protein-proteinases control biomineralization in living organisms, thereby triggering bionanomorphic mineralization with enamel structure to repair dental hard tissue defects (both enamel and dentin) [161]. Moreover, our group has found that other organic matrices, such as HA modification, can enhance $Ca^{2+}$ binding capacity by reducing the electronegativity of the collagen surface, thereby producing a local higher supersaturation and significantly promoting intrafibrillar collagen mineralization [162]. These findings offer a physicochemical perspective of the regulatory effect of polymers in BOICs and offer promising prospects for ideal materials for tooth restoration. In recent years, a bionic organic–inorganic composite has been produced for tooth repair by guiding the formation of CPO in BC nanofibers (Fig. 5(d)) [163]. The prepared composite exhibits a tensile strength of up to 1168.1 ± 10.2 MPa and a toughness of 34.1 ± 0.8 $MJ·m^{-3}$, and has potential application in tooth repair. Moreover, a composite with structure and properties similar to natural enamel was designed by using amorphous interphase-coated HAP nanowires as the inorganic phase and PVA as the binder, and is also expected to become a new generation of restorative materials for teeth [124]. The prepared composite with high stiffness (105 GPa), high hardness (5.9 GPa), high viscoelasticity (5.5 GPa), high strength (143 MPa), and high toughness (7.4 $MPa·m^{-2}$) is superior to previously reported enamel-like composites such as tooth enamel, bone, and mother-of-pearl in shells, which fully reflect the importance of material microstructure design for the improvement of material properties.

Clinical translation of BOICs for hard tissue repair has already been achieved in several cases. Bio-Oss® Collagen, a clinically approved composite consisting of deproteinized bovine bone mineral and collagen, is one of the most widely used BOICs in periodontal regeneration and maxillofacial bone augmentation [164]. Clinical studies have demonstrated its excellent osteoconductivity, favorable biocompatibility, and stable clinical outcomes in maxillary bone healing, alveolar ridge preservation, and periodontal bone regeneration. For instance, it significantly enhanced bone gap filling and mineralized bone formation after LeFort I osteotomy, demonstrating a clear clinical benefit in promoting reliable bone union compared with untreated sites. However, its limitations include slow degradation, lack of intrinsic osteoinductivity, and insufficient mechanical strength for load-bearing applications, which restrict its use in large or highly stressed bone defects. CaP/collagen bone cements represent another class of clinically applied BOICs for bone defect repair [165]. These materials exhibit good injectability, *in situ* hardening ability, and satisfactory short-term bone defect stabilization. Radiological follow-up demonstrated satisfactory bone consolidation and progressive resorption of the cement over 6–12 months, with the new bone tissue gradually replacing the cement [166]. Nevertheless, their brittleness, limited tensile strength, and imperfect matching between degradation rate and new bone formation remain major challenges for long-term functional repair.

### 5.2 Soft tissue repair

Soft tissues such as cartilage, tendons, and ligaments have anisotropic structural characteristics. Tendons and ligaments are tough and firmly fixed to bones, but they cannot regenerate spontaneously *in vivo* once injured. Tough scaffolds and hydrogels developed in recent years are a promising alternative for soft tissues [167]. By combining the features of the semi-permeability of the scaffolds and hydrogels, the high osteoconductivity of HAP and the dynamic nature of the bone tissues, the prepared BOICs have been demonstrated to exhibit great potential in soft tissue repair. Compared with hard tissue repair, the clinical translation of BOICs for soft tissue regeneration is more limited, but several BOICs have shown promising clinical relevance. A hierarchically ordered scaffold prepared by combining HAP and polymers can be used for ligament regeneration via enhanced expression of ligament-specific proteins like tenomodulin and tenascin C (Fig. 6(b)) [168]. The scaffold is composed of oppositely charged pectin and poly-D-lysine polymers, and a HAP mineral gradient is strategically introduced near both ends of the scaffold to enhance interface integration. The synergistic combination of the bionic structure,

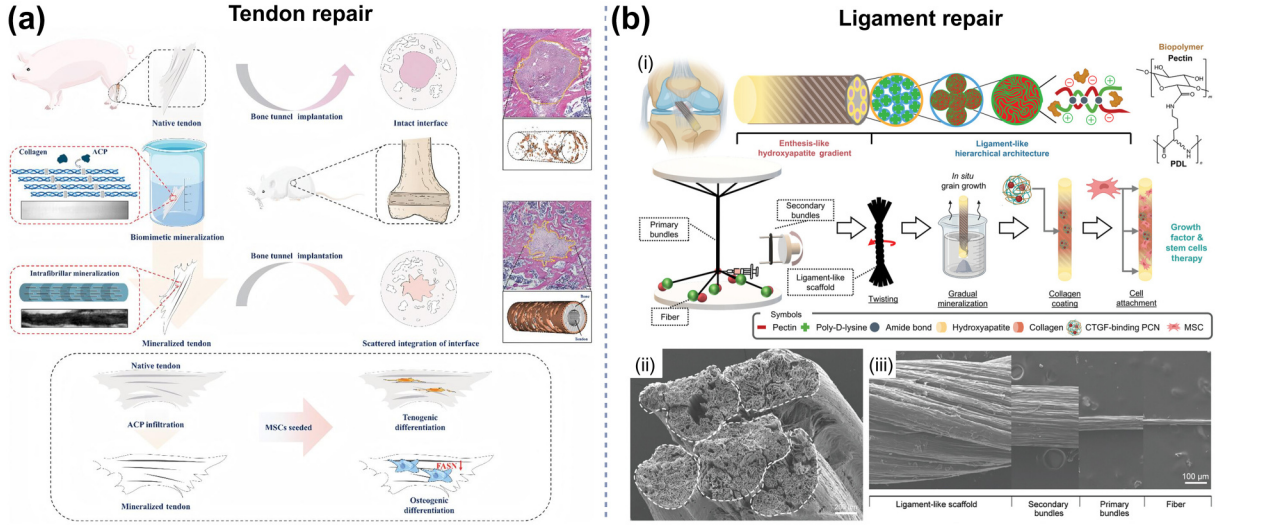


**Figure 6** Functional applications of BOICs in soft tissue repair. (a) Schematic overview for the process of bionic mineralized tendon slices fabrication and bone tunnel implantation. Reproduced with permission from ref. [170], © Chen, Y. W. et al. 2023. (b) Application of BOICs in ligament repair: (i) schematic illustration and fabrication process of the ligament-like scaffold, (ii) SEM image of the cross-section scaffold, highlighting the secondary fiber bundles with a dash line, (iii) SEM images of the fibers observed at each collection step from fibers to fiber bundles. Reproduced with permission from Ref. [168], © Wiley-VCH GmbH 2024.

gradient mineralization, and excellent biomechanical behavior positioned this ligamentous substitute as a highly attractive candidate for ligament rupture repair. Other organic components, such as collagen and PVA, are also frequently combined with CaP to construct BOICs for soft tissue repair. A muscle-like composite with high strength and high toughness mechanical properties (strength of 17.84 MPa, fracture energy of 8.97 $kJ \cdot m^{-2}$) prepared by inducing the polymerization of CPO into the PVA molecular chain network has provided a novel tactic for the design and manufacture of soft tissue repair materials [169]. In recent years, a new mineralized tendon implant with properties similar to those of native bone by infiltrating ACP precursors into collagen fibrils was synthesized (Fig. 6(a)) [170]. It leads to HAP deposition along the *c*-axis, facilitating the integration of the tendon-bone interface and generating a serrated interface *in vivo*, ultimately promoting tendon repair.

### 5.3 Simultaneous repair of hard and soft tissues

In the above article, we described the applications of BOICs in hard and soft tissue repair respectively, but it is sometimes unable to meet certain clinical demands, such as periodontitis and traumatic injuries, that require simultaneous repair of hard and soft tissues. With the development of 3D printing technology in tissue regeneration engineering, BOICs designed for the simultaneous repair of hard and soft tissues have also been extensively reported and investigated in preclinical studies. A periodontally-ordered bilayer nanostructured scaffolding material was prepared for periodontium repair (Fig. 7(a)) [171]. Porous intrafibrillar mineralized collagen (IMC) scaffolds were fabricated from collagen fibrils and n-HAP by the self-assembly technique, and further constructed bionic ordered bilayer concentrated growth factor (CGF)/IMC nano-scaffolding material by micro-embossing technique, which could recruit and regulate the multidirectional differentiation of autologous stem cells to achieve synergistic regeneration of periodontal soft and hard tissues by activating the transforming growth factor β1/Smad3 signaling pathway. Similarly, another recent study has developed a hierarchical bilayer scaffold by integrating a CS layer and an intrafibrillarly mineralized collagen layer via directional freezing and biomimetic mineralization [172]. The CS layer mimics the aligned fibers of the periodontal ligament (PDL), providing the necessary topographical cues to direct the differentiation of mesenchymal stem cells (MSCs) into PDL-like cells that form oriented collagen fibers, while a mild zinc-ion-mediated microenvironment was introduced to further support PDL-oriented matrix formation. Meanwhile, the mineralized collagen layer replicates the alveolar bone structure, promoting osteogenic differentiation of bone marrow mesenchymal stem cells (BMSCs) and supporting bone regeneration. Overall, this bilayer scaffold closely mimics the complex hierarchical architecture of the periodontal tissues, thus exhibiting great promise for synchronized periodontal hard and soft tissue regeneration. In addition, a "hard tissue ink" consisting of collagen, CS, n-HAP, and MSCs was first developed and found that it produced hard tissue by generating pluripotent cells of bone, cartilage, and bone marrow fat in the bone marrow at the same time. They then went on to use droplet 3D printing to deposit collagen and fibrinogen to achieve the simultaneous repair of skin and bone damage (Fig. 7(b)) [173]. The construction of BOICs with biological functions and hierarchically ordered structures of articular cartilage and subchondral bone is also the key to achieving high-quality osteochondral defect repair. It has been reported that the adherence capacity and osteogenic differentiation of BMSCs are greatly enhanced in the presence of n-HAP-coated scaffolds. Thus, organic materials with excellent plasticity and biocompatibility, such as gelatin, CS, and alginate, are often utilized to combine with HAP to fabricate BOICs for engineering analogs of osteochondral tissues. A hierarchical osteochondral scaffold that consisted of PCL and HAP was constructed [95]. The scaffold exhibited an excellent biocompatibility to support cell adhesion and proliferation *in vitro*, and a superior mechanical performance (compression modulus and compressive strength of 8.7 and 4.6 MPa, respectively) to provide suitable mechanical support to avoid collapse of newly formed tissues, while promoting the osteochondral regeneration. Furthermore, by using N-acryloyl glycinamide, N-[tris(hydroxymethyl)methyl] acrylamide, and β-tricalcium phosphate as raw materials, a novel scaffold was synthesized

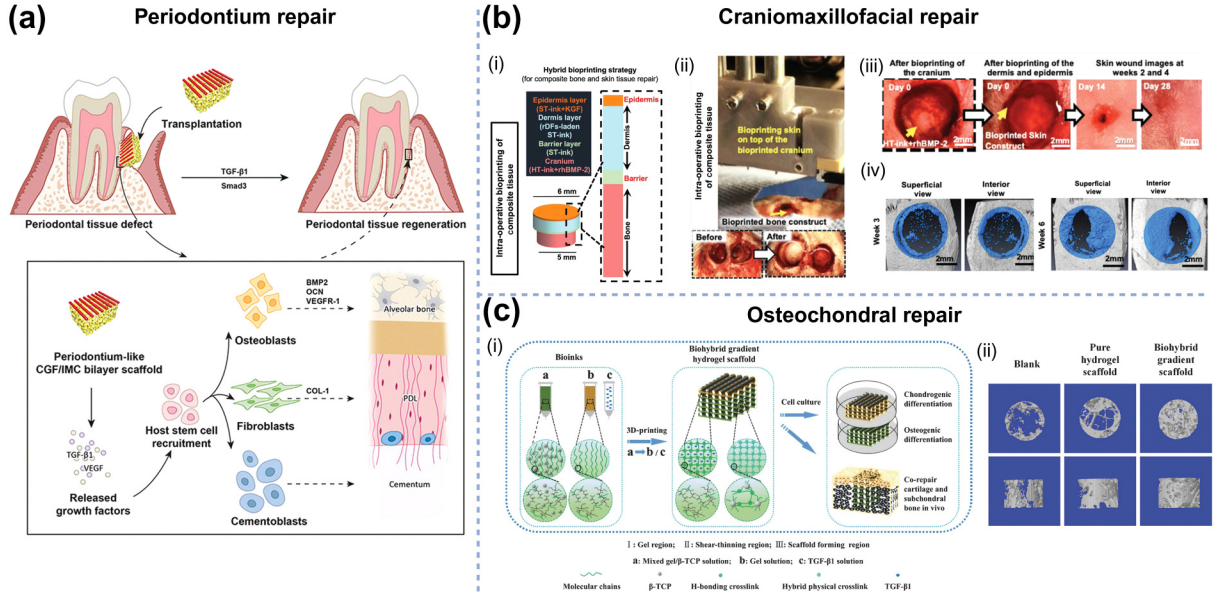


**Figure 7** Functional applications of BOICs in hard and soft tissues repair. (a) Schematic overview of the hierarchical CGF/IMC bilayer scaffold for periodontium repair. Reproduced with permission from Ref. [171], © Yu, M. et al. 2022. (b) Application of BOICs in craniomaxillofacia repair: (i) intra-operative bioprinting of composite tissues, (ii) stratified bioprinting in a rat model, (iii) representative images of skin wound repair, (iv) micro-CT evaluation of bone regeneration. Reproduced with permission from Ref. [173], © Wiley-VCH GmbH 2021. (c) Application of BOICs in osteochondral repair: (i) schematic illustration of the biohybrid gradient scaffolds, (ii) micro-CT analysis showed improved subchondral bone repair. Reproduced with permission from Ref. [174], © WILEY-VCH Verlag GmbH & Co. KGaA, Weinheim 2018.

through 3D printing (Fig. 7(c)) [174]. The prepared scaffold promoted the attachment, spreading, and chondrogenic and osteogenic differentiation of human bone marrow mesenchymal stem cells *in vitro*, thus can be used for osteochondral repair. Recently, an n-HAP and liposomes-coated integral bilayer scaffold with a porous architecture was also designed for osteochondral repair [175]. The bilayer scaffold could regenerate a cartilage-bone integrated tissue with seamless interfacial integration and offer new therapeutic opportunities for osteochondral defects, but the molecular regulatory mechanisms need to be further explored.

## 6 Summary and prospect

Biomineralization is a multifactorial process through which organisms utilize biologically controlled mechanisms to form hierarchically ordered structured organic–inorganic composites with remarkable functions [7, 176]. In recent years, scientists have investigated the induced effects of various organic matrices on inorganic minerals and used bionic mineralization to construct BOICs with excellent properties and hierarchically ordered structures. Numerous BOICs prepared by bionic mineralization strategies exhibited unparalleled advantages over traditional synthetic composites and have been successfully applied in tissue regeneration engineering with rapid development [177, 178]. Previous understandings of bionic organic–inorganic composites primarily emphasized ingredient bionics. Currently, in addition to mimicking the composition of natural minerals, researchers are increasingly focusing on the construction of their bionic hierarchically ordered structures, such as bionic bone synthesized by 3D printing [103, 159].

Despite extensive scientific research on BOICs and their integration into tissue regeneration engineering applications, achieving an ideal replication of the pristine hierarchically ordered structures and the inherent physical and chemical properties of biominerals, as well as their clinical translation and application, remains fraught with significant challenges. The perspectives for BOICs in tissue regeneration engineering are shown as follows:

**(1) Design of hierarchically ordered structures**: More stable and functional ultra-small size inorganic units should be explored to achieve precise control over the polymerization of organic and inorganic molecules and ions so as to regulate the hierarchically ordered structural assembly of BOICs. Additionally, a deeper understanding of the complex hierarchically ordered structures and interactions of BOICs should be focused. To further comprehend these complex structures, future work should employ a suite of advanced techniques. *In situ* spectroscopy and microscopy (e.g., cryo-transmission electron microscopy) reveal dynamic structural evolution; Multi-scale simulations, from quantum mechanics to finite element analysis, decipher interactions and predict properties; while synchrotron X-rays and neutron scattering probe buried interfaces, providing a holistic view from molecular to macroscopic scales.

**(2) Integration of high mechanical strength with excellent biocompatibility of BOICs**: Combining biodegradability and mechanical properties within one material is still challenging, especially for biodegradable and biocompatible substrates, which are usually polymers with excellent biocompatibility and relatively weak mechanical strength. Traditional designs that often focus on a single aspect, and are unable to simultaneously provide synergistic benefits by simultaneously addressing mechanical support and biological signaling requirements, which is the key to the medical application of BOICs. On the one hand, more efficient strategies for mineralizing natural organic chains should be explored to improve mechanical strength, controlling the mineralization process by adding additives. On the other hand, natural and synthetic organic polymer composites or artificially synthesized organic raw materials with biodegradability and compatibility are expected to be used in fabricating BOICs. A prime example is the emerging PU, whose

mechanical properties, degradation rates, and bioactivity can be precisely tailored, making it a highly promising candidate as the organic matrix for next-generation BOICs [73]. Importantly, inorganic units with ultra-small size mentioned above are also effective in enhancing the interfacial interactions of the two phases, ultimately improving the strength and toughness properties of BOICs [43].

**(3) Focus on the molecular mechanisms of BOICs interacting with cells in the biological microenvironment**: The mechanism of BOICs to promote tissue repair and regeneration in organisms is ambiguous, which may be limited by the biological properties of the bioinspired materials [152]. Consequently, advancements in the investigation of relevant mechanisms and the exploration of relevant methodologies can guide the optimization of the material properties (e.g., structure, mechanical strength, degradation rate) and significantly enhance the practical applications of BOICs. Accordingly, researchers can utilize the existing single-cell sequencing, RNA-seq, and other technical methods to obtain a more in-depth and comprehensive understanding of the process and mechanism of effect on cell behavior, thereby enabling the fabrication of bioinspired materials that fully mimic natural ones.

**(4) Preclinical translational applications**: To date, several BOICs have achieved clinical translation, including CaP/collagen bone cements for bone repair and Bio-Oss® Collagen for bone and dental repair [164, 165]. Clinically, these products have demonstrated favorable outcomes in promoting osteoconduction, providing structural support, and facilitating bone repair. However, existing clinically-translated BOICs still exhibit limitations that require improvement, including suboptimal degradation rates that may not fully synchronize with new bone formation, limited mechanical strength for load-bearing applications, long-term biological safety, and the complexity and reproducibility in manufacturing. To address these challenges, future initiatives should focus on improving material stability, controlling degradation kinetics, and optimizing composite formulations to enhance both biological and mechanical performance. Moreover, emphasizing practicality by streamlining the production process and utilizing Food and Drug Administration-approved raw materials will be crucial for ensuring safety and regulatory compliance. Preclinical applications play a vital role in bridging laboratory research and tissue regeneration engineering applications. Additionally, researchers should prioritize the clinical translation of their work by undertaking essential preclinical and clinical trials. This requires rigorous testing of biocompatibility, efficacy, and safety in large animal models to predict human responses. This stage is vital for de-risking clinical trials, ensuring patient safety, and securing regulatory approval.

## Data availability

No data was used for the research described in the article.

## Acknowledgements

This work was financially supported by the National Natural Science Foundation of China (No. 22207097), the Exploration R&D Program of Stomatological Hospital Affiliated to Zhejiang University School of Medicine (No. RD2023JCYL07), and the Key R&D Program of Zhejiang Province (No. 2024C03081) Medical Interdisciplinary Innovation Program 2024, Zhejiang University School of Medicine, the Funds of the Central Government Guiding Local Science and Technology Development (No. 2023ZY1060), and the Funds of Zhejiang Clinovation Pride.

## Declaration of competing interest

All the contributing authors report no conflict of interests in this work.

## Author contribution statement

S. X. Z.: Writing – original draft, writing – review & editing, investigation, conceptualization. H. Y. W.: Writing – review & editing. Y. D. Y.: Writing – review & editing. J. S.: Writing – review & editing. Z. J. X.: Writing – review & editing, supervision, funding acquisition. W. J. J.: Writing – original draft, writing – review & editing, supervision, funding acquisition, conceptualization. All the authors have approved the final manuscript.

## Use of AI statement

None.

## References

[1] Huang, W.; Restrepo, D.; Jung, J. Y.; Su, F. Y.; Liu, Z. Q.; Ritchie, R. O.; McKittrick, J.; Zavattieri, P.; Kisailus, D. Multiscale toughening mechanisms in biological materials and bioinspired designs. *Adv. Mater.* **2019**, *31*, 1901561.

[2] Cusack, M.; Freer, A. Biomineralization: Elemental and organic influence in carbonate systems. *Chem. Rev.* **2008**, *108*, 4433–4454.

[3] Wegst, U. G. K.; Bai, H.; Saiz, E.; Tomsia, A. P.; Ritchie, R. O. Bioinspired structural materials. *Nat. Mater.* **2015**, *14*, 23–36.

[4] Finnemore, A.; Cunha, P.; Shean, T.; Vignolini, S.; Guldin, S.; Oyen, M.; Steiner, U. Biomimetic layer-by-layer assembly of artificial nacre. *Nat. Commun.* **2012**, *3*, 966.

[5] Shao, C. Y.; Jin, B.; Mu, Z.; Lu, H.; Zhao, Y. Q.; Wu, Z. F.; Yan, L. M.; Zhang, Z. S.; Zhou, Y. C.; Pan, H. H. et al. Repair of tooth enamel by a biomimetic mineralization frontier ensuring epitaxial growth. *Sci. Adv.* **2019**, *5*, eaaw9569.

[6] Mann, S.; Archibald, D. D.; Didymus, J. M.; Douglas, T.; Heywood, B. R.; Meldrum, F. C.; Reeves, N. J. Crystallization at inorganic–organic interfaces: Biominerals and biomimetic synthesis. *Science* **1993**, *261*, 1286–1292.

[7] Yao, S. S.; Jin, B.; Liu, Z. M.; Shao, C. Y.; Zhao, R. B.; Wang, X. Y.; Tang, R. K. Biomineralization: From material tactics to biological strategy. *Adv. Mater.* **2017**, *29*, 1605903.

[8] Fang, W. F.; Mu, Z.; He, Y.; Kong, K. R.; Jiang, K.; Tang, R. K.; Liu, Z. M. Organic–inorganic covalent-ionic molecules for elastic ceramic plastic. *Nature* **2023**, *619*, 293–299.

[9] Zhu, S. H.; Wang, S.; Huang, Y. F.; Tang, Q. Y.; Fu, T. Q.; Su, R. Y.; Fan, C. Y.; Xia, S.; Lee, P. S.; Lin, Y. H. Bioinspired structural hydrogels with highly ordered hierarchical orientations by flow-induced alignment of nanofibrils. *Nat. Commun.* **2024**, *15*, 118.

[10] Liu, Y.; Luo, D.; Wang, T. Hierarchical structures of bone and bioinspired bone tissue engineering. *Small* **2016**, *12*, 4611–4632.

[11] He, Y.; Fang, W. F.; Tang, R. K.; Liu, Z. M. Controllable polymerization of inorganic ionic oligomers for precise nanostructural construction in materials. *ACS Nano* **2025**, *19*, 6648–6662.

[12] Yu, Y. D.; Kong, K. R.; Tang, R. K.; Liu, Z. M. A bioinspired ultratough composite produced by integration of inorganic ionic oligomers within polymer networks. *ACS Nano* **2022**, *16*, 7926–7936.

[13] Liu, Z. M.; Shao, C. Y.; Jin, B.; Zhang, Z. S.; Zhao, Y. Q.; Xu, X. R.; Tang, R. K. Crosslinking ionic oligomers as conformable precursors

to calcium carbonate. *Nature* **2019**, *574*, 394–398.
[14] Palmer, L. C.; Newcomb, C. J.; Kaltz, S. R.; Spoerke, E. D.; Stupp, S. I. Biomimetic systems for hydroxyapatite mineralization inspired by bone and enamel. *Chem. Rev.* **2008**, *108*, 4754–4783.
[15] Aazmi, A.; Zhang, D.; Mazzaglia, C.; Yu, M. F.; Wang, Z.; Yang, H. Y.; Huang, Y. Y. S.; Ma, L. Biofabrication methods for reconstructing extracellular matrix mimetics. *Bioact. Mater.* **2024**, *31*, 475–496.
[16] Zhong, Z. Y.; Wu, X. D.; Wang, Y. F.; Li, M. D.; Li, Y.; Liu, X. L.; Zhang, X.; Lan, Z. Y.; Wang, J. L.; Du, Y. Y. et al. Zn/Sr dual ions-collagen co-assembly hydroxyapatite enhances bone regeneration through procedural osteo-immunomodulation and osteogenesis. *Bioact. Mater.* **2022**, *10*, 195–206.
[17] Eder, M.; Amini, S.; Fratzl, P. Biological composites-complex structures for functional diversity. *Science* **2018**, *362*, 543–547.
[18] Vasquez-Sancho, F.; Abdollahi, A.; Damjanovic, D.; Catalan, G. Flexoelectricity in bones. *Adv. Mater.* **2018**, *30*, 1705316.
[19] Aizenberg, J.; Weaver, J. C.; Thanawala, M. S.; Sundar, V. C.; Morse, D. E.; Fratzl, P. Skeleton of *Euplectella* sp: Structural hierarchy from the nanoscale to the macroscale. *Science* **2005**, *309*, 275–278.
[20] Poundarik, A. A.; Boskey, A.; Gundberg, C.; Vashishth, D. Biomolecular regulation, composition and nanoarchitecture of bone mineral. *Sci. Rep.* **2018**, *8*, 1191.
[21] Nair, A. K.; Gautieri, A.; Chang, S. W.; Buehler, M. J. Molecular mechanics of mineralized collagen fibrils in bone. *Nat. Commun.* **2013**, *4*, 1724.
[22] Porter, M. M.; McKittrick, J.; Meyers, M. A. Biomimetic Materials by Freeze Casting. *JOM* **2013**, *65*, 720–727.
[23] Meyers, M. A.; Chen, P. Y.; Lin, A. Y. M.; Seki, Y. Biological materials: Structure and mechanical properties. *Prog. Mater. Sci.* **2008**, *53*, 1–206.
[24] Yeom, B.; Sain, T.; Lacevic, N.; Bukharina, D.; Cha, S. H.; Waas, A. M.; Arruda, E. M.; Kotov, N. A. Abiotic tooth enamel. *Nature* **2017**, *543*, 95–98.
[25] Kinney, J. H.; Habelitz, S.; Marshall, S. J.; Marshall, G. W. The importance of intrafibrillar mineralization of collagen on the mechanical properties of dentin. *J. Dent. Res.* **2003**, *82*, 957–961.
[26] Ding, C. M.; Chen, Z. X.; Li, J. S. From molecules to macrostructures: Recent development of bioinspired hard tissue repair. *Biomater. Sci.* **2017**, *5*, 1435–1449.
[27] Zhang, Y. R.; Du, W.; Zhou, X. D.; Yu, H. Y. Review of research on the mechanical properties of the human tooth. *Int. J. Oral Sci.* **2014**, *6*, 61–69.
[28] Arola, D. D.; Reprogel, R. K. Tubule orientation and the fatigue strength of human dentin. *Biomaterials* **2006**, *27*, 2131–2140.
[29] Koons, G. L.; Diba, M.; Mikos, A. G. Materials design for bone-tissue engineering. *Nat. Rev. Mater.* **2020**, *5*, 584–603.
[30] Place, E. S.; George, J. H.; Williams, C. K.; Stevens, M. M. Synthetic polymer scaffolds for tissue engineering. *Chem. Soc. Rev.* **2009**, *38*, 1139–1151.
[31] Sharma, A.; Kokil, G. R.; He, Y.; Lowe, B.; Salam, A.; Altalhi, T. A.; Ye, Q. S.; Kumeria, T. Inorganic/organic combination: Inorganic particles/polymer composites for tissue engineering applications. *Bioact. Mater.* **2023**, *24*, 535–550.
[32] Ajili, W.; Tovani, C. B.; Fouassier, J.; De Frutos, M.; Laurent, G. P.; Bertani, P.; Djediat, C.; Marin, F.; Auzoux-Bordenave, S.; Azaïs, T. et al. Inorganic phosphate in growing calcium carbonate abalone shell suggests a shared mineral ancestral precursor. *Nat. Commun.* **2022**, *13*, 1496.
[33] Jarcho, M.; Bolen, C. H.; Thomas, M. B.; Bobick, J.; Kay, J. F.; Doremus, R. H. Hydroxylapatite synthesis and characterization in dense polycrystalline form. *J. Mater. Sci.* **1976**, *11*, 2027–2035.
[34] Ribeiro, C. C.; Barrias, C. C.; Barbosa, M. A. Calcium phosphate-alginate microspheres as enzyme delivery matrices. *Biomaterials* **2004**, *25*, 4363–4373.
[35] Maia, M. T.; Luz, É. P. C. G.; Andrade, F. K.; Rosa, M. D. F.; Borges, M. D. F.; Arcanjo, M. R. A.; Vieira, R. S. Advances in bacterial cellulose/strontium apatite composites for bone applications. *Polym. Rev.* **2021**, *61*, 736–764.
[36] Stoehr, L. C.; Gonzalez, E.; Stampfl, A.; Casals, E.; Duschl, A.; Puntes, V.; Oostingh, G. J. Shape matters: Effects of silver nanospheres and wires on human alveolar epithelial cells. *Part. Fibre Toxicol.* **2011**, *8*, 36.
[37] Liu, X.; Miao, Y. L.; Liang, H. F.; Diao, J. J.; Hao, L. J.; Shi, Z. F.; Zhao, N. R.; Wang, Y. J. 3D-printed bioactive ceramic scaffolds with biomimetic micro/nano-HAp surfaces mediated cell fate and promoted bone augmentation of the bone-implant interface *in vivo*. *Bioact. Mater.* **2022**, *12*, 120–132.
[38] Abels, M.; Alkildani, S.; Pröhl, A.; Xiong, X.; Krastev, R.; Korzinskas, T.; Stojanovic, S.; Jung, O.; Najman, S.; Barbeck, M. The granule size mediates the *in vivo* foreign body response and the integration behavior of bone substitutes. *Materials* **2021**, *14*, 7372.
[39] Lei, C.; Wang, K. Y.; Ma, Y. X.; Hao, D. X.; Zhu, Y. N.; Wan, Q. Q.; Zhang, J. S.; Tay, F. R.; Mu, Z.; Niu, L. N. Biomimetic self-maturation mineralization system for enamel repair. *Adv. Mater.* **2024**, *36*, e2311659.
[40] Huang, X. G.; Andina, D.; Ge, J. S.; Labarre, A.; Leroux, J. C.; Castagner, B. Characterization of calcium phosphate nanoparticles based on a PEGylated chelator for gene delivery. *ACS Appl. Mater. Interfaces* **2017**, *9*, 10435–10445.
[41] Niu, L. N.; Jee, S. E.; Jiao, K.; Tonggu, L.; Li, M.; Wang, L. G.; Yang, Y. D.; Bian, J. H.; Breschi, L.; Jang, S. S. et al. Collagen intrafibrillar mineralization as a result of the balance between osmotic equilibrium and electroneutrality. *Nat. Mater.* **2017**, *16*, 370–378.
[42] Ma, Z. Q.; Li, B. K.; Tang, R. K. Biomineralization: Biomimetic synthesis of materials and biomimetic regulation of organisms. *Chin. J. Chem.* **2021**, *39*, 2071–2082.
[43] Yu, Y. D.; Mu, Z.; Jin, B.; Liu, Z. M.; Tang, R. K. Organic–inorganic copolymerization for a homogenous composite without an interphase boundary. *Angew. Chem., Int. Ed.* **2020**, *59*, 2071–2075.
[44] Yu, Y. D.; He, Y.; Mu, Z.; Zhao, Y. Q.; Kong, K. R.; Liu, Z. M.; Tang, R. K. Biomimetic mineralized organic–inorganic hybrid macrofiber with spider silk-like supertoughness. *Adv. Funct. Mater.* **2020**, *30*, 1908556.
[45] Wang, Y.; Azaïs, T.; Robin, M.; Vallée, A.; Catania, C.; Legriel, P.; Pehau-Arnaudet, G.; Babonneau, F.; Giraud-Guille, M. M.; Nassif, N. The predominant role of collagen in the nucleation, growth, structure and orientation of bone apatite. *Nat. Mater.* **2012**, *11*, 724–733.
[46] Oosterlaken, B. M.; Vena, M. P.; De With, G. *In vitro* mineralization of collagen. *Adv. Mater.* **2021**, *33*, 2004418.
[47] Ji, D.; Park, J. M.; Oh, M. S.; Nguyen, T. L.; Shin, H.; Kim, J. S.; Kim, D.; Park, H. S.; Kim, J. Superstrong, superstiff, and conductive alginate hydrogels. *Nat. Commun.* **2022**, *13*, 3019.
[48] Lee, K. Y.; Mooney, D. J. Alginate: Properties and biomedical applications. *Prog. Polym. Sci.* **2012**, *37*, 106–126.
[49] Salama, A. Cellulose/calcium phosphate hybrids: New materials for biomedical and environmental applications. *Int. J. Biol. Macromol.* **2019**, *127*, 606–617.
[50] Sun, B. J.; Lin, J. B.; Wang, T.; Liu, M. D.; Yang, L.; Ma, B.; Chaudhary, J. P.; Chen, C. T.; Sun, D. P. Gas assisted *in situ* biomimetic mineralization of bacterial cellulose/calcium carbonate bio composites by bacterial. *Int. J. Biol. Macromol.* **2021**, *182*, 1690–1696.
[51] Sozcu, S.; Frajova, J.; Wiener, J.; Venkataraman, M.; Tomkova, B.; Militky, J. Effect of drying methods on the thermal and mechanical behavior of bacterial cellulose aerogel. *Gels* **2024**, *10*, 474.
[52] Graça, M. F. P.; Miguel, S. P.; Cabral, C. S. D.; Correia, I. J. Hyaluronic acid-based wound dressings: A review. *Carbohydr.*

*Polym.* **2020**, *241*, 116364.
[53] Vasi, A. M.; Popa, M. I.; Butnaru, M.; Dodi, G.; Verestiuc, L. Chemical functionalization of hyaluronic acid for drug delivery applications. *Mater. Sci. Eng. C* **2014**, *38*, 177–185.
[54] Zhou, Z. W.; Li, H. P.; Wang, K. K.; Guo, Q.; Li, C. Z.; Jiang, H. L.; Hu, Y. Q.; Oupicky, D.; Sun, M. J. Bioreducible cross-linked hyaluronic acid/calcium phosphate hybrid nanoparticles for specific delivery of siRNA in melanoma tumor therapy. *ACS Appl. Mater. Interfaces* **2017**, *9*, 14576–14589.
[55] Jiménez-Gómez, C. P.; Cecilia, J. A. Chitosan: A natural biopolymer with a wide and varied range of applications. *Molecules* **2020**, *25*, 3981.
[56] Shariatinia, Z. Carboxymethyl chitosan: Properties and biomedical applications. *Int. J. Biol. Macromol.* **2018**, *120*, 1406–1419.
[57] Liu, X. Y.; Wu, Y. X.; Zhao, X. C.; Wang, Z. K. Fabrication and applications of bioactive chitosan-based organic–inorganic hybrid materials: A review. *Carbohydr. Polym.* **2021**, *267*, 118179.
[58] Di Martino, A.; Sittinger, M.; Risbud, M. V. Chitosan: A versatile biopolymer for orthopaedic tissue-engineering. *Biomaterials* **2005**, *26*, 5983–5990.
[59] Liu, G. F.; Xia, P. C.; Li, B. K.; Qiao, T. H.; Wu, Q. L.; Sarfraz, M. H.; Sun, Y.; Ouyang, H. W.; He, Y. Strong and tough tendon-mimetic silk fibroin for tissue regeneration. *Adv. Healthc. Mater.* **2025**, *14*, 2500428.
[60] Sorushanova, A.; Delgado, L. M.; Wu, Z. N.; Shologu, N.; Kshirsagar, A.; Raghunath, R.; Mullen, A. M.; Bayon, Y.; Pandit, A.; Raghunath, M. et al. The collagen suprafamily: From biosynthesis to advanced biomaterial development. *Adv. Mater.* **2019**, *31*, 1801651.
[61] Ko, E.; Lee, J. S.; Kim, H.; Yang, S. Y.; Yang, D.; Yang, K.; Lee, J.; Shin, J.; Yang, H. S.; Ryu, W. et al. Electrospun silk fibroin nanofibrous scaffolds with two-stage hydroxyapatite functionalization for enhancing the osteogenic differentiation of human adipose-derived mesenchymal stem cells. *ACS Appl. Mater. Interfaces* **2018**, *10*, 7614–7625.
[62] Si, J. H.; Cui, Z. X.; Wang, Q. T.; Liu, Q.; Liu, C. T. Biomimetic composite scaffolds based on mineralization of hydroxyapatite on electrospun poly(ε-caprolactone)/nanocellulose fibers. *Carbohydr. Polym.* **2016**, *143*, 270–278.
[63] Gaaz, T. S.; Sulong, A. B.; Akhtar, M. N.; Kadhum, A. A. H.; Mohamad, A. B.; Al-Amiery, A. A. Properties and applications of polyvinyl alcohol, halloysite nanotubes and their nanocomposites. *Molecules* **2015**, *20*, 22833–22847.
[64] Seifi, S.; Shamloo, A.; Barzoki, A. K.; Bakhtiari, M. A.; Zare, S.; Cheraghi, F.; Peyrovan, A. Engineering biomimetic scaffolds for bone regeneration: Chitosan/alginate/polyvinyl alcohol-based double-network hydrogels with carbon nanomaterials. *Carbohydr. Polym.* **2024**, *339*, 122232.
[65] Lu, J. X.; Sun, C. Y.; Yang, K. X.; Wang, K. L.; Jiang, Y. Y.; Tusiime, R.; Yang, Y.; Fan, F.; Sun, Z. Y.; Liu, Y. et al. Properties of polylactic acid reinforced by hydroxyapatite modified nanocellulose. *Polymers* **2019**, *11*, 1009.
[66] Li, X.; Liu, C.; Wang, S. Y.; Jiao, J.; Di, D. H.; Jiang, T. Y.; Zhao, Q. F.; Wang, S. L. Poly(acrylic acid) conjugated hollow mesoporous carbon as a dual-stimuli triggered drug delivery system for chemo-photothermal synergistic therapy. *Mater. Sci. Eng. C* **2017**, *71*, 594–603.
[67] Wang, L. S.; Duan, L.; Liu, G.; Sun, J. F.; Shahbazi, M. A.; Kundu, S. C.; Reis, R. L.; Xiao, B.; Yang, X. Bioinspired polyacrylic acid-based dressing: Wet adhesive, self-healing, and multi-biofunctional coacervate hydrogel accelerates wound healing. *Adv. Sci.* **2023**, *10*, 2207352.
[68] Li, F.; Xing, Q. G.; Han, Y. C.; Li, Y.; Wang, W.; Perera, T. S. H.; Dai, H. L. Ultrasonically assisted preparation of poly(acrylic acid)/calcium phosphate hybrid nanogels as pH-responsive drug carriers. *Mater. Sci. Eng. C* **2017**, *80*, 688–697.
[69] Kurtz, S. M.; Devine, J. N. PEEK biomaterials in trauma, orthopedic, and spinal implants. *Biomaterials* **2007**, *28*, 4845–4869.
[70] Sailaja, G. S.; Sreenivasan, K.; Yokogawa, Y.; Kumary, T. V.; Varma, H. K. Bioinspired mineralization and cell adhesion on surface functionalized poly(vinyl alcohol) films. *Acta Biomater.* **2009**, *5*, 1647–1655.
[71] Gao, X. S.; Wang, H. H.; Luan, S. F.; Zhou, G. Y. Low-temperature printed hierarchically porous induced-biomineralization polyarylether ketone scaffold for bone tissue engineering. *Adv. Healthc. Mater.* **2022**, *11*, e2200977.
[72] Dang, G. P.; Gu, J. T.; Song, J. H.; Li, Z. T.; Hao, J. X.; Wang, Y. Z.; Wang, C. Y.; Ye, T.; Zhao, F.; Zhang, Y. F. et al. Multifunctional polyurethane materials in regenerative medicine and tissue engineering. *Cell Rep. Phys. Sci.* **2024**, *5*, 102053.
[73] Asefnejad, A.; Behnamghader, A.; Khorasani, M. T.; Farsadzadeh, B. Polyurethane/fluor-hydroxyapatite nanocomposite scaffolds for bone tissue engineering Part I: Morphological, physical, and mechanical characterization. *Int. J. Nanomedicine* **2011**, *6*, 93–100.
[74] Ma, P. X. Biomimetic materials for tissue engineering. *Adv. Drug Deliv. Rev.* **2008**, *60*, 184–198.
[75] O'Brien, F. J. Biomaterials & scaffolds for tissue engineering. *Mater. Today* **2011**, *14*, 88–95.
[76] Ji, T. J.; Feng, B.; Shen, J.; Zhang, M.; Hu, Y. Q.; Jiang, A. X.; Zhu, D. Q.; Chen, Y. W.; Ji, W.; Zhang, Z. et al. An avascular niche created by axitinib-loaded PCL/collagen nanofibrous membrane stabilized subcutaneous chondrogenesis of mesenchymal stromal cells. *Adv. Sci.* **2021**, *8*, 2100351.
[77] Liu, Y. K.; Von Witzleben, M.; Duin, S.; Bernhardt, A.; Gelinsky, M. Topology-optimized melt-electrowritten PCL patch for abdominal wall reconstruction. *Bioact. Mater.* **2026**, *55*, 529–545.
[78] Hoemann, C. D.; Rodríguez González, J.; Guzmán-Morales, J.; Chen, G. P.; Jalali Dil, E.; Favis, B. D. Chitosan coatings with distinct innate immune bioactivities differentially stimulate angiogenesis, osteogenesis and chondrogenesis in poly-caprolactone scaffolds with controlled interconnecting pore size. *Bioact. Mater.* **2022**, *10*, 430–442.
[79] Tan, H. P.; Chu, C. R.; Payne, K. A.; Marra, K. G. Injectable *in situ* forming biodegradable chitosan-hyaluronic acid based hydrogels for cartilage tissue engineering. *Biomaterials* **2009**, *30*, 2499–2506.
[80] Svensson, A.; Nicklasson, E.; Harrah, T.; Panilaitis, B.; Kaplan, D. L.; Brittberg, M.; Gatenholm, P. Bacterial cellulose as a potential scaffold for tissue engineering of cartilage. *Biomaterials* **2005**, *26*, 419–431.
[81] Cui, T. T.; Yu, J. F.; Li, Q.; Wang, C. F.; Chen, S.; Li, W. J.; Wang, G. F. Large-scale fabrication of robust artificial skins from a biodegradable sealant-loaded nanofiber scaffold to skin tissue via microfluidic blow-spinning. *Adv. Mater.* **2020**, *32*, 2000982.
[82] Guo, Y. Z.; Han, Y.; Cao, Y. Y.; Chen, Y. P.; Xie, J. W.; Ding, H. C.; Liang, S. F.; Liu, X.; Sun, W. J.; Tang, J. B. et al. Facile fabrication of tough super macroporous hydrogel via enhanced phase separation. *Adv. Funct. Mater.* **2025**, *35*, 2412412.
[83] Niu, X. F.; Feng, Q. L.; Wang, M. B.; Guo, X. D.; Zheng, Q. X. Porous nano-HA/collagen/PLLA scaffold containing chitosan microspheres for controlled delivery of synthetic peptide derived from BMP-2. *J. Control. Release* **2009**, *134*, 111–117.
[84] Stevens, M. M. Biomaterials for bone tissue engineering. *Mater. Today* **2008**, *11*, 18–25.
[85] Guo, C.; Wu, J. C.; Zeng, Y. M.; Li, H. Construction of 3D bioprinting of HAP/collagen scaffold in gelation bath for bone tissue engineering. *Regen. Biomater.* **2023**, *10*, rbad067.
[86] Qi, Y. P.; Cheng, Z.; Ye, Z.; Zhu, H. L.; Aparicio, C. Bioinspired mineralization with hydroxyapatite and hierarchical naturally aligned nanofibrillar cellulose. *ACS Appl. Mater. Interfaces* **2019**, *11*, 27598–27604.
[87] Li, C. X.; Born, A. K.; Schweizer, T.; Zenobi-Wong, M.; Cerruti, M.; Mezzenga, R. Amyloid-hydroxyapatite bone biomimetic composites. *Adv. Mater.* **2014**, *26*, 3207–3212.

[88] Wan, F. Q.; Ping, H.; Wang, W. X.; Zou, Z. Y.; Xie, H.; Su, B. L.; Liu, D. B.; Fu, Z. Y. Hydroxyapatite-reinforced alginate fibers with bioinspired dually aligned architectures. *Carbohydr. Polym.* **2021**, *267*, 118167.

[89] Cheng, Z.; Ye, Z.; Natan, A.; Ma, Y.; Li, H. Y.; Chen, Y.; Wan, L. Q.; Aparicio, C.; Zhu, H. L. Bone-inspired mineralization with highly aligned cellulose nanofibers as template. *ACS Appl. Mater. Interfaces* **2019**, *11*, 42486–42495.

[90] Jiang, S. J.; Wang, M. H.; Wang, Z. Y.; Gao, H. L.; Chen, S. M.; Cong, Y. H.; Yang, L.; Wen, S. M.; Cheng, D. D.; He, J. C. et al. Radially porous nanocomposite scaffolds with enhanced capability for guiding bone regeneration *in vivo*. *Adv. Funct. Mater.* **2022**, *32*, 2110931.

[91] Liang, R. J.; Li, R.; Mo, W. D.; Zhang, X. Z.; Ye, J. C.; Xie, C.; Li, W. Y.; Peng, Z.; Gu, Y. Q.; Huang, Y. X. et al. Engineering biomimetic silk fibroin hydrogel scaffolds with "organic–inorganic assembly" strategy for rapid bone regeneration. *Bioact. Mater.* **2024**, *40*, 541–556.

[92] Yang, T.; Hao, Z. C.; Wu, Z. Z.; Xu, B. X.; Liu, J. C.; Fan, L.; Wang, Q. M.; Li, Y. S.; Li, D. Y.; Tang, S. Z. et al. An engineered lamellar bone mimicking full-scale hierarchical architecture for bone regeneration. *Bioact. Mater.* **2023**, *27*, 181–199.

[93] Chen, D. Y.; Liu, P.; Li, M. N.; Zhang, C. Q.; Gao, Y. S.; Guo, Y. P. Nacre-mimetic hydroxyapatite/chitosan/gelatin layered scaffolds modifying substance P for subchondral bone regeneration. *Carbohydr. Polym.* **2022**, *291*, 119575.

[94] Kim, J. W.; Han, Y. S.; Lee, H. M.; Kim, J. K.; Kim, Y. J. Effect of morphological characteristics and biomineralization of 3D-printed gelatin/hyaluronic acid/hydroxyapatite composite scaffolds on bone tissue regeneration. *Int. J. Mol. Sci.* **2021**, *22*, 6794.

[95] Du, Y. Y.; Liu, H. M.; Yang, Q.; Wang, S.; Wang, J. L.; Ma, J.; Noh, I.; Mikos, A. G.; Zhang, S. M. Selective laser sintering scaffold with hierarchical architecture and gradient composition for osteochondral repair in rabbits. *Biomaterials* **2017**, *137*, 37–48.

[96] Yu, M. H.; Feng, L.; Gan, Z. L.; Hua, Y. C.; Wu, H. Y.; Ganss, B.; Yang, H. M. Tubular nanoclay-enhanced calcium phosphate mineralization and assembly to impart high stiffness and antimicrobial properties. *ACS Appl. Mater. Interfaces* **2024**, *16*, 9190–9200.

[97] Wang, W. Z.; Zhang, B. Q.; Li, M. X.; Li, J.; Zhang, C. Y.; Han, Y. L.; Wang, L.; Wang, K. F.; Zhou, C. C.; Liu, L. et al. 3D printing of PLA/n-HA composite scaffolds with customized mechanical properties and biological functions for bone tissue engineering. *Compos. Part B: Eng* **2021**, *224*, 109192.

[98] Yuan, B.; Wang, L. N.; Zhao, R.; Yang, X.; Yang, X.; Zhu, X. D.; Liu, L. M.; Zhang, K.; Song, Y. M.; Zhang, X. D. A biomimetically hierarchical polyetherketoneketone scaffold for osteoporotic bone repair. *Sci. Adv.* **2020**, *6*, eabc4704.

[99] Geng, X. W.; Tang, Y. F.; Yuan, B.; Dai, Y. Y.; Yu, H. P.; Xiong, Z. C.; Zhu, Y. J.; Chen, X. S. Biomimetically ordered ultralong hydroxyapatite nanowires-based hierarchical hydrogel scaffold with osteoimmunomodulatory and osteogenesis abilities for augmenting bone regeneration. *Chem. Eng. J.* **2024**, *488*, 151136.

[100] Song, P.; Gui, X. Y.; Wu, L. N.; Su, X. Y.; Zhou, W. Z.; Luo, Z. Y.; Zhang, B. Q.; Feng, P.; Wei, W.; Fan, C. et al. DLP fabrication of multiple hierarchical biomimetic GelMA/SilMA/HAp scaffolds for enhancing bone regeneration. *Biomacromolecules* **2024**, *25*, 1871–1886.

[101] Wang, J.; Wu, Y.; Li, G. F.; Zhou, F. J.; Wu, X.; Wang, M. M.; Liu, X. R.; Tang, H.; Bai, L.; Geng, Z. et al. Engineering large-scale self-mineralizing bone organoids with bone matrix-inspired hydroxyapatite hybrid bioinks. *Adv. Mater.* **2024**, *36*, 2309875.

[102] Cui, X.; Xu, L. L.; Shan, Y. Z.; Li, J. X.; Ji, J. Y.; Wang, E. G.; Zhang, B. K.; Wen, X. Z.; Bai, Y.; Luo, D. et al. Piezocatalytically-induced controllable mineralization scaffold with bone-like microenvironment to achieve endogenous bone regeneration. *Sci. Bull.* **2024**, *69*, 1895–1908.

[103] Zhang, K. X.; Fang, H. W.; Cheng, X. Y.; Li, J. Y.; Zeng, J. J.; Zhang, T.; Cui, H. Y.; Gu, H. J.; Yin, J. B. Biomimetic fibrous bone substitute manufacture through non-solvent-assisted 3D printing. *Adv. Funct. Mater.* **2025**, *35*, 2419464.

[104] Wang, T.; Zhai, Y. K.; Nuzzo, M.; Yang, X. C.; Yang, Y. P.; Zhang, X. P. Layer-by-layer nanofiber-enabled engineering of biomimetic periosteum for bone repair and reconstruction. *Biomaterials* **2018**, *182*, 279–288.

[105] Ma, P. F.; Wu, W. J.; Wei, Y.; Ren, L.; Lin, S. X.; Wu, J. H. Biomimetic gelatin/chitosan/polyvinyl alcohol/nano-hydroxyapatite scaffolds for bone tissue engineering. *Mater. Des.* **2021**, *207*, 109865.

[106] Wang, Y. L.; Zhou, X. Y.; Jiang, J. H.; Zhao, T. H.; Dang, J. B.; Hu, R. B.; Shen, C.; Fan, Q. C.; Sun, D. H.; Zhang, M. Carboxymethyl chitosan-enhanced multi-level microstructured composite hydrogel scaffolds for bone defect repair. *Carbohydr. Polym.* **2025**, *348*, 122847.

[107] Zhang, C. W.; Si, M. Q.; Chen, C.; He, P.; Fei, Z. Q.; Xu, N.; He, X. M. Hierarchical engineering for biopolymer-based hydrogels with tailored property and functionality. *Adv. Mater.* **2025**, *37*, 2414897.

[108] Wang, Y. Y.; Jiang, X. Y.; Li, X. S.; Ding, K. X.; Liu, X. R.; Huang, B.; Ding, J. J.; Qu, K. Y.; Sun, W. Z.; Xue, Z. X. et al. Bionic ordered structured hydrogels: Structure types, design strategies, optimization mechanism of mechanical properties and applications. *Mater. Horiz.* **2023**, *10*, 4033–4058.

[109] Whitesides, G. M.; Mathias, J. P.; Seto, C. T. Molecular self-assembly and nanochemistry: A chemical strategy for the synthesis of nanostructures. *Science* **1991**, *254*, 1312–1319.

[110] Yang, R. L.; Zhu, Y. J.; Chen, F. F.; Qin, D. D.; Xiong, Z. C. Bioinspired macroscopic ribbon fibers with a nacre-mimetic architecture based on highly ordered alignment of ultralong hydroxyapatite nanowires. *ACS Nano* **2018**, *12*, 12284–12295.

[111] Yu, X.; Kong, K. R.; Ma, X. M.; Yu, Y. D.; Shen, Y. L.; Sang, Y. H.; Wang, J.; Shen, S. D.; Xu, X. R.; Liu, Z. M. et al. Organic–inorganic copolymerization induced oriented crystallization for robust lightweight porous composite. *Small* **2024**, *20*, 2403443.

[112] Wu, X. Y.; Yang, H. Y.; Liu, G. F.; Sun, W.; Li, J. Y.; Zhao, Y. N.; Gao, X.; Liu, X. Z.; Song, F. F.; Wang, S. L. et al. Osteomimix: A multidimensional biomimetic cascade strategy for bone defect repair. *Adv. Mater.* **2025**, *37*, 2416715.

[113] Podsiadlo, P.; Kaushik, A. K.; Arruda, E. M.; Waas, A. M.; Shim, B. S.; Xu, J. D.; Nandivada, H.; Pumplin, B. G.; Lahann, J.; Ramamoorthy, A. et al. Ultrastrong and stiff layered polymer nanocomposites. *Science* **2007**, *318*, 80–83.

[114] Podsiadlo, P.; Tang, Z. Y.; Shim, B. S.; Kotov, N. A. Counterintuitive effect of molecular strength and role of molecular rigidity on mechanical properties of layer-by-layer assembled nanocomposites. *Nano Lett.* **2007**, *7*, 1224–1231.

[115] Greiner, A.; Wendorff, J. H. Electrospinning: A fascinating method for the preparation of ultrathin fibers. *Angew. Chem., Int. Ed.* **2007**, *46*, 5670–5703.

[116] Holzwarth, J. M.; Ma, P. X. Biomimetic nanofibrous scaffolds for bone tissue engineering. *Biomaterials* **2011**, *32*, 9622–9629.

[117] Zhou, Y. S.; Deng, J. J.; Zhang, Y.; Li, C.; Wei, Z.; Shen, J. L.; Li, J. J.; Wang, F.; Han, B.; Chen, D. et al. Engineering DNA-guided hydroxyapatite bulk materials with high stiffness and outstanding antimicrobial ability for dental inlay applications. *Adv. Mater.* **2022**, *34*, 2202180.

[118] Kundu, K.; Afshar, A.; Katti, D. R.; Edirisinghe, M.; Katti, K. S. Composite nanoclay-hydroxyapatite-polymer fiber scaffolds for bone tissue engineering manufactured using pressurized gyration. *Compos. Sci. Technol.* **2021**, *202*, 108598.

[119] Shi, S.; Si, Y. F.; Han, Y. T.; Wu, T.; Iqbal, M. I.; Fei, B.; Li, R. K. Y.; Hu, J. L.; Qu, J. P. Recent progress in protective membranes

fabricated via electrospinning: Advanced materials, biomimetic structures, and functional applications. *Adv. Mater.* **2022**, *34*, 2107938.
[120] Deville, S.; Saiz, E.; Nalla, R. K.; Tomsia, A. P. Freezing as a path to build complex composites. *Science* **2006**, *311*, 515–518.
[121] Munch, E.; Launey, M. E.; Alsem, D. H.; Saiz, E.; Tomsia, A. P.; Ritchie, R. O. Tough, bio-inspired hybrid materials. *Science* **2008**, *322*, 1516–1520.
[122] Joukhdar, H.; Seifert, A.; Jüngst, T.; Groll, J.; Lord, M. S.; Rnjak-Kovacina, J. Ice templating soft matter: Fundamental principles and fabrication approaches to tailor pore structure and morphology and their biomedical applications. *Adv. Mater.* **2021**, *33*, 2100091.
[123] Bai, H.; Chen, Y.; Delattre, B.; Tomsia, A. P.; Ritchie, R. O. Bioinspired large-scale aligned porous materials assembled with dual temperature gradients. *Sci. Adv.* **2015**, *1*, e1500849.
[124] Zhao, H. W.; Liu, S. J.; Wei, Y.; Yue, Y. H.; Gao, M. R.; Li, Y. B.; Zeng, X. L.; Deng, X. L.; Kotov, N. A.; Guo, L. et al. Multiscale engineered artificial tooth enamel. *Science* **2022**, *375*, 551–556.
[125] Shao, G. F.; Hanaor, D. A. H.; Shen, X. D.; Gurlo, A. Freeze casting: From low-dimensional building blocks to aligned porous structures—A review of novel materials, methods, and applications. *Adv. Mater.* **2020**, *32*, 1907176.
[126] Zhang, H. F.; Hussain, I.; Brust, M.; Butler, M. F.; Rannard, S. P.; Cooper, A. I. Aligned two- and three-dimensional structures by directional freezing of polymers and nanoparticles. *Nat. Mater.* **2005**, *4*, 787–793.
[127] Guo, X.; Dong, X. Y.; Zou, G. J.; Gao, H. J.; Zhai, W. Strong and tough fibrous hydrogels reinforced by multiscale hierarchical structures with multimechanisms. *Sci. Adv.* **2023**, *9*, eadf7075.
[128] Zhang, W. L.; Zhang, Y. W.; Dai, Y.; Xia, F.; Zhang, X. J. Gradient adhesion modification of polyacrylamide/alginate-calcium tough hydrogels. *J. Mater. Chem. B* **2022**, *10*, 757–764.
[129] Wu, L.; Kang, Y.; Shi, X. Y.; Yuezhen, B.; Qu, M. J.; Li, J. Y.; Wu, Z. S. Natural-wood-inspired ultrastrong anisotropic hybrid hydrogels targeting artificial tendons or ligaments. *ACS Nano* **2023**, *17*, 13522–13532.
[130] De Santis, M. M.; Alsafadi, H. N.; Tas, S.; Bölükbas, D. A.; Prithiviraj, S.; Da Silva, I. A. N.; Mittendorfer, M.; Ota, C.; Stegmayr, J.; Daoud, F. et al. Extracellular-matrix-reinforced bioinks for 3D bioprinting human tissue. *Adv. Mater.* **2021**, *33*, 2005476.
[131] Khoonkari, M.; Es Sayed, J.; Oggioni, M.; Amirsadeghi, A.; Dijkstra, P.; Parisi, D.; Kruyt, F.; Van Rijn, P.; Włodarczyk-Biegun, M. K.; Kamperman, M. Bioinspired processing: Complex coacervates as versatile inks for 3D bioprinting. *Adv. Mater.* **2023**, *35*, 2210769.
[132] Pawar, A. A.; Saada, G.; Cooperstein, I.; Larush, L.; Jackman, J. A.; Tabaei, S. R.; Cho, N. J.; Magdassi, S. High-performance 3D printing of hydrogels by water-dispersible photoinitiator nanoparticles. *Sci. Adv.* **2016**, *2*, e1501381.
[133] Zhou, F. F.; Hong, Y.; Liang, R. J.; Zhang, X. Z.; Liao, Y. G.; Jiang, D. M.; Zhang, J. Y.; Sheng, Z. X.; Xie, C.; Peng, Z. et al. Rapid printing of bio-inspired 3D tissue constructs for skin regeneration. *Biomaterials* **2020**, *258*, 120287.
[134] Highley, C. B.; Song, K. H.; Daly, A. C.; Burdick, J. A. Jammed microgel inks for 3D printing applications. *Adv. Sci.* **2019**, *6*, 1801076.
[135] Zhang, H.; Huang, H. F.; Hao, G. R.; Zhang, Y. S.; Ding, H.; Fan, Z. J.; Sun, L. Y. 3D printing hydrogel scaffolds with nanohydroxyapatite gradient to effectively repair osteochondral defects in Rats. *Adv. Funct. Mater.* **2021**, *31*, 2006697.
[136] Shen, H. Y.; Xing, F.; Shang, S. Y.; Jiang, K.; Kuzmanović, M.; Huang, F. W.; Liu, Y.; Luo, E.; Edeleva, M.; Cardon, L. et al. Biomimetic mineralized 3D-printed polycaprolactone scaffold induced by self-adaptive nanotopology to accelerate bone regeneration. *ACS Appl. Mater. Interfaces* **2024**, *16*, 18658–18670.
[137] Hospodiuk, M.; Dey, M.; Sosnoski, D.; Ozbolat, I. T. The bioink: A comprehensive review on bioprintable materials. *Biotechnol. Adv.* **2017**, *35*, 217–239.
[138] Cai, Y. L.; Chang, S. Y.; Gan, S. W.; Ma, S.; Lu, W. F.; Yen, C. C. Nanocomposite bioinks for 3D bioprinting. *Acta Biomater.* **2022**, *151*, 45–69.
[139] Zheng, Z. Z.; Eglin, D.; Alini, M.; Richards, G. R.; Qin, L.; Lai, Y. X. Visible light-induced 3D bioprinting technologies and corresponding bioink materials for tissue engineering: A review. *Engineering* **2021**, *7*, 966–978.
[140] Wüst, S.; Godla, M. E.; Müller, R.; Hofmann, S. Tunable hydrogel composite with two-step processing in combination with innovative hardware upgrade for cell-based three-dimensional bioprinting. *Acta Biomater.* **2014**, *10*, 630–640.
[141] Rodell, C. B.; MacArthur, J. W.; Dorsey, S. M.; Wade, R. J.; Wang, L. L.; Woo, Y. J.; Burdick, J. A. Shear-thinning supramolecular hydrogels with secondary autonomous covalent crosslinking to modulate viscoelastic properties *in vivo*. *Adv. Funct. Mater.* **2015**, *25*, 636–644.
[142] Chen, H. Z.; Shen, M. D.; Shen, J.; Li, Y. F.; Wang, R.; Ye, M. H.; Li, J. F.; Zhong, C.; Bao, Z. N.; Yang, X. Y. et al. A new injectable quick hardening anti-collapse bone cement allows for improving biodegradation and bone repair. *Biomater. Adv.* **2022**, *141*, 213098.
[143] Wang, H. C.; Tian, J. J.; Jiang, Y. X.; Liu, S.; Zheng, J. C.; Li, N. Y.; Wang, G. Y.; Dong, F.; Chen, J. Y.; Xie, Y. et al. A 3D biomimetic optoelectronic scaffold repairs cranial defects. *Sci. Adv.* **2023**, *9*, eabq7750.
[144] Tang, S. X.; Dong, Z. Y.; Ke, X.; Luo, J.; Li, J. S. Advances in biomineralization-inspired materials for hard tissue repair. *Int. J. Oral Sci.* **2021**, *13*, 42.
[145] Pina, S.; Oliveira, J. M.; Reis, R. L. Natural-based nanocomposites for bone tissue engineering and regenerative medicine: A review. *Adv. Mater.* **2015**, *27*, 1143–1169.
[146] Li, Z. W.; Du, T. M.; Ruan, C. S.; Niu, X. F. Bioinspired mineralized collagen scaffolds for bone tissue engineering. *Bioact. Mater.* **2021**, *6*, 1491–1511.
[147] Nassif, N.; Gobeaux, F.; Seto, J.; Belamie, E.; Davidson, P.; Panine, P.; Mosser, G.; Fratzl, P.; Giraud Guille, M. M. Self-assembled collagen-apatite matrix with bone-like hierarchy. *Chem. Mater.* **2010**, *22*, 3307–3309.
[148] De Melo Pereira, D.; Habibovic, P. Biomineralization-inspired material design for bone regeneration. *Adv. Healthc. Mater.* **2018**, *7*, 1800700.
[149] Wang, X. F.; Fang, J.; Zhu, W. W.; Zhong, C. X.; Ye, D. D.; Zhu, M. Y.; Lu, X.; Zhao, Y. S.; Ren, F. Z. Bioinspired highly anisotropic, ultrastrong and stiff, and osteoconductive mineralized wood hydrogel composites for bone repair. *Adv. Funct. Mater.* **2021**, *31*, 2010068.
[150] Liu, Y.; Liu, S.; Luo, D.; Xue, Z. J.; Yang, X. N.; Gu, L.; Zhou, Y. H.; Wang, T. Hierarchically staggered nanostructure of mineralized collagen as a bone-grafting scaffold. *Adv. Mater.* **2016**, *28*, 8740–8748.
[151] Zhou, H. J.; Lee, J. Nanoscale hydroxyapatite particles for bone tissue engineering. *Acta Biomater.* **2011**, *7*, 2769–2781.
[152] Pei, Y. F.; Wang, Y. H.; Chen, J. X.; Zhou, J.; Han, Y. Z.; Liu, X. Y.; Chen, S. Y.; Chen, S.; He, D. X.; Wu, Y. X. et al. Bionic nanostructures create mechanical signals to mediate the composite structural bone regeneration through multi-system regulation. *Adv. Sci.* **2025**, *12*, e02299.
[153] Dupont, S.; Morsut, L.; Aragona, M.; Enzo, E.; Giulitti, S.; Cordenonsi, M.; Zanconato, F.; Le Digabel, J.; Forcato, M.; Bicciato, S. et al. Role of YAP/TAZ in mechanotransduction. *Nature* **2011**, *474*, 179–183.
[154] Werner, M.; Blanquer, S. B. G.; Haimi, S. P.; Korus, G.; Dunlop, J. W. C.; Duda, G. N.; Grijpma, D. W.; Petersen, A. Surface curvature differentially regulates stem cell migration and differentiation via

altered attachment morphology and nuclear deformation. *Adv. Sci.* **2017**, *4*, 1600347.
[155] Shayan, M.; Padmanabhan, J.; Morris, A. H.; Cheung, B.; Smith, R.; Schroers, J.; Kyriakides, T. R. Nanopatterned bulk metallic glass-based biomaterials modulate macrophage polarization. *Acta Biomater.* **2018**, *75*, 427–438.
[156] Yuan, B.; Cheng, Q. W.; Zhao, R.; Zhu, X. D.; Yang, X.; Yang, X.; Zhang, K.; Song, Y. M.; Zhang, X. D. Comparison of osteointegration property between PEKK and PEEK: Effects of surface structure and chemistry. *Biomaterials* **2018**, *170*, 116–126.
[157] Yuan, B.; Zhang, Y. X.; Zhao, R.; Lin, H.; Yang, X.; Zhu, X. D.; Zhang, K.; Mikos, A. G.; Zhang, X. D. A unique biomimetic modification endows polyetherketoneketone scaffold with osteoinductivity by activating cAMP/PKA signaling pathway. *Sci. Adv.* **2022**, *8*, eabq7116.
[158] Winter, G. D.; Simpson, B. J. Heterotopic bone formed in a synthetic sponge in the skin of young pigs. *Nature* **1969**, *223*, 88–90.
[159] Shi, Y.; Shi, J.; Sun, Y.; Liu, Q. Q.; Zhang, C.; Shao, C. Y.; Yu, K.; Ge, M. J.; Mi, R.; Gu, J. Y. et al. A hierarchical 3D graft printed with nanoink for functional craniofacial bone restoration. *Adv. Funct. Mater.* **2023**, *33*, 2301099.
[160] Robin, M.; Mouloungui, E.; Castillo Dali, G.; Wang, Y.; Saffar, J. L.; Pavon-Djavid, G.; Divoux, T.; Manneville, S.; Behr, L.; Cardi, D. et al. Mineralized collagen plywood contributes to bone autograft performance. *Nature* **2024**, *636*, 100–107.
[161] Zhou, Q. L.; Guo, M. X.; Zhang, Q. L.; Li, Q. L.; Cao, C. Y. On-site smart biomimetic mineralization of starch-templated CaP prenucleation clusters triggered by α-amylase. *Mater. Des.* **2021**, *210*, 110093.
[162] Wu, H. Y.; Shao, C. Y.; Shi, J.; Hu, Z. H.; Zhou, Y. Y.; Chen, Z.; Tang, R. K.; Xie, Z. J.; Jin, W. J. Hyaluronic acid-mediated collagen intrafibrillar mineralization and enhancement of dentin remineralization. *Carbohydr. Polym.* **2023**, *319*, 121174.
[163] Zhao, X.; Chen, Z. H.; Zhuo, H.; Zhong, C. Y.; Shi, G.; Liu, T. L.; Huang, X. F.; Zhong, L. X.; Peng, X. W. Ultra-strong and transparent biomimetic nanocomposite through orientation effects and *in situ* biomineralization. *Adv. Funct. Mater.* **2024**, *34*, 2310094.
[164] Rohner, D.; Hailemariam, S.; Hammer, B. Le Fort I osteotomies using Bio-Oss® collagen to promote bony union: A prospective clinical split-mouth study. *Int. J. Oral Max. Surg.* **2013**, *42*, 585–591.
[165] Ryu, K. S.; Shim, J. H.; Heo, H. Y.; Park, C. K. Therapeutic efficacy of injectable calcium phosphate cement in osteoporotic vertebral compression fractures: Prospective nonrandomized controlled study at 6-month follow-up. *World Neurosurg.* **2010**, *73*, 408–411.
[166] Libicher, M.; Hillmeier, J.; Liegibel, U.; Sommer, U.; Pyerin, W.; Vetter, M.; Meinzer, H. P.; Grafe, I.; Meeder, P.; Nöldge, G. et al. Osseous integration of calcium phosphate in osteoporotic vertebral fractures after kyphoplasty: Initial results from a clinical and experimental pilot study. *Osteoporos. Int.* **2006**, *17*, 1208–1215.
[167] Nonoyama, T.; Wada, S.; Kiyama, R.; Kitamura, N.; Mredha, M. T. I.; Zhang, X.; Kurokawa, T.; Nakajima, T.; Takagi, Y.; Yasuda, K. et al. Double-network hydrogels strongly bondable to bones by spontaneous osteogenesis penetration. *Adv. Mater.* **2016**, *28*, 6740–6745.
[168] Liu, Y. C.; Chen, S. H.; Kuan, C. H.; Chen, S. H.; Huang, W. Y.; Chen, H. X.; Wang, T. W. Assembly of interfacial polyelectrolyte complexation fibers with mineralization gradient for physiologically-inspired ligament regeneration. *Adv. Mater.* **2024**, *36*, 2314294.
[169] Yu, Y. D.; Kong, K. R.; Mu, Z.; Zhao, Y. Q.; Liu, Z. M.; Tang, R. K. Muscle-like ultratough hybrid hydrogel constructed by heterogeneous inorganic polymerization on an organic network. *ACS Appl. Mater. Interfaces* **2020**, *12*, 54212–54221.
[170] Chen, Y. W.; Zhang, Y. X.; Chen, X. Y.; Huang, J. Y.; Zhou, B.; Zhang, T.; Yin, W.; Fang, C. L.; Yin, Z.; Pan, H. H. et al. Biomimetic intrafibrillar mineralization of native tendon for soft–hard interface integration by infiltration of amorphous calcium phosphate precursors. *Adv. Sci.* **2023**, *10*, 2304216.
[171] Yu, M.; Luo, D.; Qiao, J.; Guo, J. S.; He, D. Q.; Jin, S. S.; Tang, L.; Wang, Y.; Shi, X.; Mao, J. et al. A hierarchical bilayer architecture for complex tissue regeneration. *Bioact. Mater.* **2022**, *10*, 93–106.
[172] Qin, W.; Li, L.; Mu, Z.; Yu, W. W.; Zhu, Y. N.; Jia, S. L.; Xuan, K.; Niu, W.; Niu, L. N. A hierarchical Bilayered scaffold for periodontal complex structure regeneration. *J. Biomed. Mater. Res.* **2025**, *113*, e37793.
[173] Moncal, K. K.; Gudapati, H.; Godzik, K. P.; Heo, D. N.; Kang, Y.; Rizk, E.; Ravnic, D. J.; Wee, H.; Pepley, D. F.; Ozbolat, V. et al. Intra-operative bioprinting of hard, soft, and hard/soft composite tissues for craniomaxillofacial reconstruction. *Adv. Funct. Mater.* **2021**, *31*, 2010858.
[174] Gao, F.; Xu, Z. Y.; Liang, Q. F.; Liu, B.; Li, H. F.; Wu, Y. H.; Zhang, Y. Y.; Lin, Z. F.; Wu, M. M.; Ruan, C. S. et al. Direct 3D printing of high strength biohybrid gradient hydrogel scaffolds for efficient repair of osteochondral defect. *Adv. Funct. Mater.* **2018**, *28*, 1706644.
[175] Zhao, W. K.; Sun, B. M.; Song, Y.; Cao, Y.; Liu, Y. C.; Zhou, D. D.; Zhou, Q.; Xie, F.; Huang, W.; Li, X. X. et al. Nanohydroxyapatite and liposomes-coated integral bilayer scaffold for osteochondral repair via mimicking the dual differentiation microenvironment of BMSCs. *Nano Mater. Sci.* **2025**, *7*, 539–554.
[176] Ma, C. Y.; Du, T. M.; Niu, X. F.; Fan, Y. B. Biomechanics and mechanobiology of the bone matrix. *Bone Res.* **2022**, *10*, 59.
[177] Zhang, Y. G.; Li, J. P.; Mouser, V. H. M.; Roumans, N.; Moroni, L.; Habibovic, P. Biomimetic mechanically strong one-dimensional hydroxyapatite/poly(D, L-lactide) composite inducing formation of anisotropic collagen matrix. *ACS Nano* **2021**, *15*, 17480–17498.
[178] Nepal, D.; Kang, S.; Adstedt, K. M.; Kanhaiya, K.; Bockstaller, M. R.; Brinson, L. C.; Buehler, M. J.; Coveney, P. V.; Dayal, K.; El-Awady, J. A. et al. Hierarchically structured bioinspired nanocomposites. *Nat. Mater.* **2023**, *22*, 18–35.